Accepted Manuscript

Geological Society, London, Special Publications

Hardground, gap and thin black shale: spatial heterogeneity of arrested carbonate sedimentation during the Jenkyns Event (T-OAE) in a Tethyan pelagic basin (Gerecse Mts, Hungary)

Tamás Müller, Gregory D. Price, Emanuela Mattioli, Máté Zs. Leskó, Ferenc Kristály & József Pálfy

DOI: https://doi.org/10.1144/SP514-2020-266

To access the most recent version of this article, please click the DOI URL in the line above. When citing this article please include the above DOI.

Received 15 December 2020
Revised 25 March 2021
Accepted 25 March 2021

Supplementary material at https://doi.org/10.6084/m9.figshare.c.5355342

Hardground, gap and thin black shale: spatial heterogeneity of arrested carbonate sedimentation during the Jenkyns Event (T-OAE) in a Tethyan pelagic basin (Gerecse Mts, Hungary)

Tamás Müller[1,2*], Gregory D. Price[3], Emanuela Mattioli[4,5], Máté Zs. Leskó[6], Ferenc Kristály[6], József Pálfy[2,7]

[1] *Isotope Climatology and Environmental Research Centre, Institute for Nuclear Research, Bem tér 18/C, H-4026, Debrecen, Hungary*

[2]*Department of Geology, Eötvös Loránd University, Pázmány Péter sétány 1/C, Budapest H-1117, Hungary*

[3]*School of Geography, Earth and Environmental Sciences, Plymouth University, Drake Circus, Plymouth, PL4 8AA, UK*

[4]*Univ Lyon1, ENSL, CNRS, LGL-TPE, F-69622, Villeurbanne, France*

[5]*Institut Universitaire de France (IUF), France*

[6]*Institute of Mineralogy and Geology, University of Miskolc, HU-3515 Miskolc-Egyetemváros, Miskolc, Hungary*

[7]*MTA-MTM-ELTE Research Group for Paleontology, POB 137, H-1431, Budapest, Hungary*

[*]Corresponding author. Email: beregond02@gmail.com

Keywords: Early Jurassic, calcification crisis, carbonate sedimentation, chemostratigraphy

Abstract

The Jenkyns Event or Toarcian Oceanic Anoxic Event (T-OAE) was an episode of severe environmental perturbations reflected in carbon isotope and other geochemical anomalies. Although well studied in the epicontinental basins in NW Europe, its effects are less understood in open marine environments. Here we present new geochemical (carbon isotope, $CaCO_3$, [Mn]) and nannofossil biostratigraphic data from the Tölgyhát and Kisgerecse sections in the Gerecse Hills (Hungary). These sections record pelagic carbonate sedimentation near the margin of the Tethys Ocean. A negative carbon isotope excursion of ~6‰ is observed in the Tölgyhát section, in a condensed clay and black shale layer where the $CaCO_3$ content drops in association with the Jenkyns Event. At Kisgerecse, bio- and chemostratigraphic data suggest a gap in the lower Toarcian. The presence of an uppermost Pliensbachian hardground, absence of the lowermost Toarcian Tenuicostatum ammonite zone, and the condensed record of the Jenkyns Event at Tölgyhát, together with a condensed Tenuicostatum Zone and the missing negative carbon isotope anomaly at Kisgerecse implies arrested carbonate sedimentation. A calcification crisis and sea-level rise together led to a decrease in carbonate production and terrigenous input, suggesting that volcanogenic CO_2-driven global warming may have been their common cause.

In the Early Jurassic, a series of severe environmental perturbations such as global warming (Suan et al., 2010), a second-order mass extinction (Caruthers et al., 2014), ocean anoxia (Pearce et al., 2008), and calcification crisis (Trecalli et al., 2012) happened in the early Toarcian (~183 Ma), collectively referred to as Toarcian Oceanic Anoxic Event (T-OAE) (Jenkyns, 1988; Jenkyns, 2010) or recently coined as the Jenkyns Event (Müller et al., 2017; Reolid et al., 2020). This time interval was characterised by enhanced marine primary production leading to the appearance of organic-rich sediments in marine and lacustrine settings under anoxic-euxinic conditions (Jenkyns, 1988; Xu et al., 2017). However, some other authors point to a high primary production occurring before the event and to a phytoplankton blackout concomitant with it (Bucefalo Palliani et al., 2002; Mattioli et al., 2009). The Jenkyns Event is coincident with a characteristic negative carbon isotope excursion (CIE) with a magnitude of ~5‰ (Hesselbo et al., 2000; Hermoso et al., 2009; Suan et al., 2015). This negative CIE is present in different substrates, e.g. marine biogenic carbonate, micrite, and in marine and terrestrial organic matter, implying a major perturbation of the carbon cycle affecting the exogenic carbon reservoirs (Suan et al., 2008a; Hermoso et al., 2009; Suan et al., 2010; Bodin et al., 2010; Hesselbo and Pieńkowski, 2011; Müller et al., 2020b). Furthermore, this carbon isotope anomaly can be also traced at multiple localities around the world suggesting a global extent of this event (Gröcke et al., 2011; Caruthers et al., 2011; Suan et al., 2011; Izumi et al., 2012; Al-Suwaidi et al., 2016). A second-order mass extinction is also associated with the Jenkyns Event severely affecting the biosphere (Caswell et al., 2009; Danise et al., 2013; Caruthers et al., 2014), with a remarkable temporal coincidence with the emplacements of the Karoo-Ferrar large igneous province (LIP) (Pálfy & Smith, 2000). The large amount of ^{12}C that triggered the negative CIE has been hypothesized to be originated from volcanic degassing of CO_2 from the Karoo-Ferrar LIP and/or thermogenic methane release from coal sediments in the Karoo Basin due to sill emplacements (McElwain et al., 2005; Svensen et al., 2007). Alternatively, methane-hydrate dissociation from marine sediments (Hesselbo et al., 2000; Kemp et al., 2005), methane release from terrestrial wetlands and/or from permafrost (Them et al., 2017; Ruebsam et al. 2019; Krencker et al. 2019), and upwelling of ^{12}C-rich bottom water and stratification of water-column (Küspert, 1982; Schouten et al., 2000) have been suggested as well. The negative CIE and CO_2 release are also coincident with global warming and a rapid temperature rise by ~7°C (Bailey et al., 2003; Suan et al., 2010). The globally elevated temperature resulted in the acceleration of the hydrological cycle, increased continental runoff and nutrient input into the ocean, further increasing primary productivity (Cohen et al., 2004; Jenkyns, 2010; Percival et al., 2016; Kemp et al., 2020). This high primary productivity led to oxygen depletion of the seawater resulting in the development of anoxic or euxinic water masses, occasionally even spreading to the photic zone (van de Schootbrugge et al., 2005; Pearce et al., 2008; Ruebsam et al., 2018). Thallium isotope studies revealed that seawater oxygen levels started to drop gradually already at the Pliensbachian/Toarcian boundary and reached euxinic conditions during the Jenkyns Event (Them et al., 2018). This is coherent with enhanced primary productivity occurring from the base of the Toarcian, followed by enhanced thermohaline stratification promoting anoxia in the core of the event (Bucefalo Palliani et al., 2002; Mattioli et al., 2009). A biocalcification crisis simultaneous with the Jenkyns Event severely affected both carbonate platforms and pelagic carbonate factories (Mattioli et al., 2009; Trecalli et al., 2012; Ettinger et al., 2021; Krencker et al., 2020; Müller et al., 2020b). Brachiopod $\delta^{11}B$-pH data imply that seawater pH started to drop, in multiple steps, already after the Pliensbachian/Toarcian boundary, reaching the minimum (~7.2; a total drop of 0.4–0.5 in pH values) immediately before and during the Jenkyns Event, that suggests a significant global lowering of seawater pH. A remarkable, rapid rise in pH at the onset of the Jenkyns Event indicates that organic carbon production and burial increased the withdrawal of atmospheric CO_2 simultaneously with the start of the negative CIE. Carbonate system modeling revealed that the pH decrease was also accompanied by a substantial drop in seawater carbonate saturation ($\Omega<1$) (Müller et al., 2020a).

In order to better assess the global extent of this chain of environmental perturbations related to the Jenkyns Event oceanic records would be necessary but little oceanic crust of Toarcian age is preserved. Therefore, pelagic successions with a depositional setting close to the open ocean have a key importance (Suan et al., 2018). So far, only a handful of such sections have been studied from the sedimentary record of the Panthalassan margin in Japan and Canada (Gröcke et al., 2011; Caruthers et al., 2011) and from the NW Tethyan margin from European sections (Jenkyns et al., 1991; Vető et al., 1997; Kafousia et al., 2011; Neumeister et al., 2015; Polgári et al., 2016; Arabas et al., 2017; Suan et al., 2018; Müller et al., 2017; 2020b).

To augment this dataset and to improve our understanding of the local and regional differences in the processes and expression of the Jenkyns Event, here we present new high-resolution carbon isotope, $CaCO_3$ and [Mn] geochemical data, nannofossil biostratigraphy and mineralogical information from two sections, Tölgyhát and Kisgerecse from the Gerecse Hills in north-central Hungary. These sections are biostratigraphically well-constrained (Géczy, 1984; 1985; Kovács, 2012) and exhibit lithological variations that reflect the early Toarcian environmental and biotic changes. Paleogeographically, they represent condensed, pelagic records of the early Toarcian in an ocean-facing setting with proximity to the open Tethys Ocean (Fig. 1). Our study aims to characterize the changes in pelagic carbonate sedimentation and their relation to possible ocean acidification and calcification crisis that, compared to the extent and effects of anoxia, are lesser known components of the Jenkyns Event.

Geological background and stratigraphy

The Gerecse Hills are located in north-central Hungary, 50 km northwest of Budapest, in the northeastern part of the Transdanubian Range (Fig. 2A). In the Late Triassic, this area was located at the margin of the Tethys Ocean where the depositional environment was dominated by the extensive Dachstein carbonate platform. Regional rifting started in the latest Triassic and earliest Jurassic and later, in the Middle Jurassic, led to the opening of the Penninic Ocean. As a result, the platform was dissected and differential subsidence throughout the Early Jurassic created a depositional environment with small local basins and intervening elevated submarine highs (Császár et al., 1998). The Hettangian strata in the

Gerecse Hills are assigned to the Pisznice Limestone Formation (Fm.). The lower part of this unit is pink, thick-bedded limestone (Fig. 2B, C) that contains intraclasts and bioclasts including brachiopods and crinoids, suggesting a high-energy, shallow marine depositional environment. The upper part of the Pisznice Fm. is Sinemurian–early Pliensbachian in age and consists of more thinly bedded, red nodular pelagic limestones of *ammonitico rosso* facies with a rich brachiopod fauna (Dulai, 1998; Császár et al., 1998). The thickness of the Pisznice Fm. varies locally between 20–55 m that reflects the articulated paleotopography. Another Sinemurian formation in the Gerecse is the Hierlatz Limestone Fm. that appears as crinoid- and brachiopod-rich talus breccia or infill of neptunian dykes in older formations (i.e. the Dachstein Limestone and the Pisznice Limestone). The upper part of the Pliensbachian belongs to the Törökbükk Limestone Fm. that does not exceed a few meters in thickness and shows similar facies and depositional conditions as the Pisznice Fm. but contains abundant manganiferous nodules and intraclasts with Mn-coating and is locally crinoidal (Császár et al., 1998; Sasvári et al., 2009; Budai et al., 2018). Alternatively, this unit was assigned to the Tűzkövesárok Fm. that is also characterized by *ammonitico rosso*-type lithofacies but is more widespread farther west in the Transdanubian Range, in the Bakony Mts. The late Pliensbacian ammonite *Fuciniceras* was reported from this unit from the intensively studied section at Tata (Fülöp, 1976). The Pliensbachian-Toarcian boundary is commonly marked by an uneven, 1–2 cm thick Fe-Mn-bearing hardground or a distinct sedimentary gap at different localities. In the Bakony Mts., the Úrkút Manganese Ore Formation forms a ~40 m thick, economically significant manganese ore deposits with organic-rich black shale intercalations. This unit is considered to represent the Jenkyns Event, expressed in peculiar, temporally and spatially restricted ore-forming processes (Haas, 2012; Polgári et al., 2016; Suan et al., 2016). In the Gerecse Hills the Úrkút Fm. is only present in the Tölgyhát quarry section where it is limited to a 10–30 cm thick bed (Fig. 2B) (Konda, 1988; Sasvári et al., 2009). Although ammonites do not occur in the Úrkút Fm. in the Gerecse Hills, on the basis of facies similarities with the Úrkút locality an early Toarcian age, equivalent to the Tenuicostatum and Serpentinum Zones is assumed (Császár et al., 1998). From the Úrkút Fm. at the Tölgyhát Quarry Polgári et al. (2000) reported a single TOC measurement of 2.68 wt%. This unit is locally divided into two lithofacies, the lower half is a yellowish, thin-layered clayey marl with manganese nodules, whereas the upper half is a thin-layered organic-rich black shale. Above this unit and elsewhere in the Gerecse Hills the lower Toarcian is represented by the ~3 m thick Kisgerecse Marl Fm. This formation consists of thin-bedded red nodular pelagic marl and marly limestone (Fig. 2B, D) with a rich ammonoid fauna that indicates the presence of the Serpentinum and Bifrons Zones, proven in the studied sections by the occurrence of subzonal index taxa *Harpoceras serpentinum*, *H. falciferum*, and *Hildoceras sublevisoni* (Géczy, 1985; Kovács, 2012). At only one locality, in the Kisgerecse section, a single 5 cm thick limestone layer immediately overlying the top of the Pliensbachian Törökbükk Fm. yielded *Fontanelliceras* cf. *fontanellense*. This ammonoid species was considered diagnostic of the Tenuicostatum Zone (Géczy, 1984; 1985; Kovács, 2012) but it is now thought to have a narrow range straddling the Pliensbachian/Toarcian boundary, from the upper Emaciatum/Spinatum to lowermost Tenuicostatum zones (Meister et al., 2017). Nevertheless, with the possible exception of the Kisgerecse locality, the Tenuicostatum Zone has not been identified in any other section in the Gerecse Hills, and Toarcian successions commonly start in the Serpentinum Zone (Kovács, 2012) indicative of a hiatus. A detailed biostratigraphic study at nearby Nagy-Pisznice Hill documented that the upper part of the Kisgerecse Fm. belongs to the Gradatus Zone and the topmost bed of the formation represents the base of the overlying late Toarcian Thouarsense Zone, revealed by the occurrence of zonal index species *Merlaites gradatus* and *Grammoceras thouarsense*, respectively (Galácz et al. 2010). On top of the Kisgerecse Fm. after a distinct albeit gradual facies shift, deposition of the red nodular, *ammonitico rosso*-type pelagic limestone returns with some marly intercalations in the Tölgyhát Limestone Fm. that continues up to the Bajocian (Császár et al., 1998; Budai et al., 2018). Relationships of these Jurassic lithostratigraphic units of the study area in the Gerecse and adjacent parts of the Transdanubian Range are summarized in Fig. 3.

In this study we have investigated a 2.2 m interval in the Tölgyhát Quarry section (Fig. 2B; 4) (47°43'22.0"N; 18°30'46.7"E), covering the uppermost Pliensbachian part of the Törökbükk Fm., a ~24 cm of the Úrkút Fm. separated by a 1-5 cm thick hardground from the Törökbükk Fm. and the lower part of the Kisgerecse Fm. reaching up to the middle Toarcian Bifrons Zone. The Tölgyhát quarry exposes the most complete and expanded Jurassic section that is thought to represent a local basinal setting (Budai et al., 2018). In addition, a 2.3 m interval section excavated above the Kisgerecse quarry (Fig. 2C, D; 5) (47°41'22.6"N; 18°29'36.8"E) was investigated, covering the uppermost ~30 cm of the Törökbükk Fm. and the lower ~2 m of the Kisgerecse Fm. reaching the Bifrons Zone as well. Short accounts of these two sections, only 4 km apart, were provided by Konda (1986, 1988), whereas detailed stratigraphic results of a recently completed geological mapping project are found in Budai et al. (2018).

Methods

At both the Tölgyhát and Kisgerecse sections high-resolution sampling was carried out after detailed measurements of the target intervals of 2.2 and 2.3 m in thickness, respectively. A cordless drill with hardened steel drill bit was used to obtain rock powder for carbon and oxygen isotope ratio measurements, and major and minor element ICP-AES analyses. A total of 58 samples were collected from the Tölgyhát and 49 from the Kisgerecse sections. Sample spacing was 2 cm at the lowermost 1 m of the sections and 10 cm higher up. In addition, during a subsequent sampling campaign, 17 bulk samples were collected from the Tölgyhát section for mineral composition and XRD analyses, covering the interval between ~0.3–1.3 m. In order to improve the biostratigraphic control, 18 bulk rock samples were taken from the Tölgyhát section for nannofossil analyses.

Carbon and oxygen isotope, and ICP-AES elemental analyses were carried out at the geochemical laboratory of the University of Plymouth (UK). 200 to 500 µg of carbonate was reacted with 100% phosphoric acid and stable isotope data were generated on a VG Optima mass spectrometer with a Gilson autosampler. Carbon and oxygen isotope ratios are expressed in the internationally accepted per mil (‰) standard notation relative to the Vienna PeeDee belemnite (VPDB). Isotopic results were calibrated against the NBS-19 international standard. Reproducibility for both $\delta^{18}O$ and $\delta^{13}C$ was better than 0.2‰, based upon multiple sample analyses. ICP-AES element (Ca, Mg, Sr, Fe, Mn) analyses were carried out on a Varian 725-ES spectrometer. During the preparation procedure, subsamples of 100–200 mg were dissolved in 4% nitric acid. Based upon analysis of duplicate samples, reproducibility was better than 4% of the measured concentration of each element.

X-ray powder diffraction (XRD) measurements were carried out in the laboratories of the Institute of Mineralogy and Geology at the University of Miskolc (Hungary) using a Bruker D8 Advance diffractometer, applying Cu-Kα radiation, 40 mA tube current and 40 kV accelerating voltage, parallel beam geometry obtained with Göbel mirror in reflection geometry, Vantec-1 position-sensitive detector with 1° detector window opening and 0.007° 2θ / 14 sec goniometer speed. Identification of crystalline phases was done by the Search/Match algorithm (Marquart et al., 1979) in the DiffracPlus EVA on ICDD PDF2 (2005) database. Rietveld refinement (Bish and Post, 1993) was performed using the TOPAS4 software with empirical instrument parameterization on the NIST SRM640d Si standard, crystal structure data for calculations were obtained from the AMCSD [22] database. The <2 µm grain size fraction was separated for oriented XRD measurements by gravitational separation in a distilled water column, where the settling time was determined using Stoke's Law. From every sample, two oriented specimens were prepared and both were measured in air-dry condition. The first sample was measured after heating to 350°C and 550°C, in order to observe structural collapse. The other sample was treated with ethylene glycol using the vapor method (Brunton, 1955) to determine the swelling.

Microscope slides for calcareous nannofossil analysis were made from 18 samples. A small amount of powdered rock was mixed with water before spreading onto a cover slide as homogeneously as possible (Bown and Young, 1998). Cover slides were mounted onto microscope slides by Rhodopass B resine (polyvinyl acetate) on a hot plate. Slides were then studied using a Leica DM750P polarized microscope at 1000X magnification. As the slides revealed a very poor nannofossil content, a minimum of 3 traverses per sample were analysed (~2 mm^2). The preservation state of the nannofossils was estimated based on the degree of etching and overgrowth, according to Roth (1984). Calcareous nannofossil slides are curated at the Collections de Géologie de Lyon with a FSL number.

Results

Calcareous nannofossil biostratigraphy

The nannofossil preservation is rather poor in the samples from the Tölgyhát section. Five samples are completely barren, and four others only contain *Schizosphaerella* spp., a taxon with uncertain affinities and no biostratigraphic value. Based on the presence of *Lotharingius crucicentralis* in the sample TH5, the NJT5b subzone of Ferreira et al. (2019) is identified at 0.65 m (Fig. 2; Table 2). The overlying interval spanning the Úrkút Fm. is barren, but from 1.2 m stratigraphically upwards calcareous nannofossils are present again. Significantly, the last occurrence of *Mitrolithus jansae* is recorded at 1.60 m. This disappearance event has been recently proposed by Ferreira et al. (2019) to define the base of the NJT6b subzone, which in several sections correlates with the aftermath of Jenkyns Event. The following nannofossil event is the first occurrence of *Discorhabdus striatus*, which is considered as the marker of the NJ7, NJT7 and NJT7a zones (Bown and Cooper, 1998; Mattioli and Erba, 1999; Ferreira et al., 2019, respectively). This nannofossil zone correlates with the upper part of early Toarcian.

Stable isotope and elemental geochemistry

Bulk carbonate $\delta^{13}C$ values from both the Tölgyhát and the Kisgerecse sections show a distinct pattern. At Tölgyhát, in the Törökbükk Fm. values are gently oscillating between -1 and 2‰ (Figs. 4, 5). In the Úrkút Fm., in an interval not dated by nannofossils, a sharp negative carbon isotope excursion (CIE) of ~6.5‰ occurs within 10 cm, coincident with the change in lithology from the yellow marl to the black shale layer. The most negative value reaches -5.8‰ (Fig. 4). Above this very negative value, within the black shale layer, five samples did not yield a sufficient amount of carbonate for analyses. The next $\delta^{13}C$ value obtained immediately above the black shale near the base of the Kisgerecse Fm. captures the rebound phase of the negative CIE (-1.5‰). Above the negative CIE in the Kisgerecse Fm. the $\delta^{13}C$ curve remains nearly flat where values fall in a narrow range between 3 and 3.5‰ (Fig. 4).

At Kisgerecse the $\delta^{13}C$ record shows fluctuating values between 2.1–2.9‰ in the Pliensbachian part of the section (Fig. 5). Higher up, the $\delta^{13}C$ curve indicates a positive excursion of ~1.5‰ in the Tenuicostatum Zone and the lower half of the Serpentinum Subzone (Kovács, 2012), reaching 3.6‰. In the upper half of the Serpentinum Subzone and lower part of the Falciferum Subzone, values fluctuate between 3‰ and 4.2‰, where the latter represents the most positive value (Fig. 5). Higher in the Falciferum Subzone the $\delta^{13}C$ curve shows a slight negative trend up to the Bifrons Zone boundary, declining from 3.1 to 2.6‰. In the Bifrons Zone the $\delta^{13}C$ curve becomes nearly flat with values between 2.6 and 2.9‰ (Fig.5).

The $\delta^{18}O$ data from the Tölgyhát section show a large variability in the Törökbükk Fm. and the Úrkút Fm., where the values range between -10.4 and -1.3‰. In the Kisgerecse Fm. $\delta^{18}O$ values display less variability, within a range of 1‰, between -2.1 and -1.1‰. In the Kisgerecse section the $\delta^{18}O$ record does not show any clear trend, the values fluctuate between -1.6 and -2.6‰.

Ca ICP-AES data from both the Tölgyhát and Kisgerecse sections were used to compute calcium carbonate content, considering carbonate minerals as the prevailing phase that contains Ca. $CaCO_3$ content is varying between 55–88 wt% in the Törökbükk Fm. and subsequently drops sharply from 88 to 2.6 wt% in the Úrkút Fm., reaching the lowest values in the black shale layer (Fig. 4). Above the black shale, $CaCO_3$ rises abruptly to ~80 wt% and remains high, fluctuating between ~70 and ~83 wt% (Fig. 4). In the Kisgerecse section, there is a general decreasing trend in the $CaCO_3$ curve, where values decline from ~88 to ~50 wt% (Fig. 5).

The Sr/Ca ratio of samples from both the Tölgyhát and Kisgerecse sections is expressed in mmol/mol. Sr/Ca ratio values generally range between 0.13 and 0.44 mmol/mol in the Tölgyhát section with the exception of the black shale layer of the Úrkút Fm. where it increases suddenly to 1.85 mmol/mol and decreases to 0.24 mmol/mol at the top of the black shale layer. Remarkably, the black shale layer also provided the lowest Ca (1.4 wt%) and Sr (34 ppm) concentrations. At the Kisgerecse section the Sr/Ca ratio does not show any clear pattern, values are varying between 0.18 and 0.33 mmol/mol.

Manganese concentration data obtained from ICP-AES analyses show very high variability within the Törökbükk Fm. in the Tölgyhát section where values are between 0.15 and 1 wt%. Surprisingly, Mn concentration in the Úrkút Fm. is the lowest within the entire section (0–0.3 wt%), reaching very low values (67 ppm) in the black shale layer (Fig. 4). The only level where exceptionally high [Mn] can be expected is the hardground layer at the base of the Úrkút Fm., which was excluded from sampling because samples were taken primarily for stable isotope analyses. Higher up in the Kisgerecse Fm. Mn concentration is less variable, it remains between 0.15 and 0.27 wt% (Fig. 4). [Mn] in the Kisgerecse section is generally significantly lower than at Tölgyhát, showing higher values in the Törökbükk Fm. (0.06–0.1 wt%) and somewhat lower values in the Kisgerecse Fm. (0.03–0.06 wt%) (Fig. 5).

Mineral composition

In the Tölgyhát section, calcite content is high in the Törökbükk Fm. (84–97 wt%), drops significantly to ~50 wt% in the hardground layer that marks the base of the Úrkút Fm., and reaches the lowest values of 1–3 wt% in the yellow clay and the black shale. In the red marl at the base of the Kisgerecse Fm., calcite content increases to ~50 wt% and reaches even higher values of 85–96 wt% upsection. In the higher part of the Kisgerecse Fm. calcite content drops again to 62–66 wt% (Fig. 7). Detrital components such as quartz and clay minerals (illite, kaolinite, and randomly interstratified illite/smectite) occur in very low concentrations in the Törökbükk Fm.: the proportion of quartz ranges from 1 to 5 wt%, illite is 2 to 7 wt%. Kaolinite is only present in the uppermost part of the formation making up 2 wt%. In the Úrkút Fm., the abundance of both quartz and illite increases significantly to ~30 and ~33 to 41 wt%, respectively, whereas kaolinite remains subordinate at ~0,5–1 wt% (Fig.

7). At the base of the Kisgerecse Fm., quartz and illite concentration is high at ~12 and ~20 wt%, respectively, but they decrease higher up to 1–4 and 2-9 wt%. At the higher part of the Kisgerecse Fm. their proportion increases again to ~ 10 and ~20 wt% (Fig. 7). Other detrital components make a negligible contribution to the total mineral composition. Randomly interstratified illite/smectite and microcline make up 2–11 and 4–11 wt% of the Úrkút Fm., but they reappear in the higher part of the Kisgerecse Fm. at 1–3 wt% only. Muscovite is only present in the black shale layer of the Úrkút Fm. (~9 wt%). The hardground layer at the base of the Úrkút Fm. is distinguished by its very high proportion of pyrolusite (51 wt%).

Full details of the geochemical and mineralogical data are provided as supplementary material in Table 3.

Discussion

Effect of diagenesis

Screening for potential diagenetic overprint is important before the evaluation and a comprehensive paleoenvironmental and paleoclimatic interpretation of stable isotope data. An assessment of the relationship between carbon and oxygen isotopes in marine carbonates is often applied in order to evaluate the degree of diagenetic alteration (Brand and Veizer, 1981). Generally, a positive correlation between the two isotopic ratios is considered as a sign of the influence of meteoric water during diagenesis. However, such correlation might not represent a secondary diagenetic effect if there is no sign of subaerial exposure of sediments or the changes in $\delta^{13}C$ and $\delta^{18}O$ both record major environmental perturbations and climate change that are reflected in isotopic changes, such as the case during the Jenkyns Event (Hermoso et al., 2012; Ullmann et al., 2014; Schobben et al., 2016). Additionally, lithological changes in marine carbonate successions may display differential diagenetic alteration in $\delta^{13}C$ and $\delta^{18}O$ (Rosales et al., 2001). Therefore, we tested the correlation between carbon and oxygen isotopes, considering also the distinct lithologies of the studied sections (Table 1). At the Kisgerecse section, $\delta^{13}C$ and $\delta^{18}O$ values indicate no significant correlation in the Törökbükk Fm. (Pearson r = 0.03) and in the Kisgerecse Fm. (Pearson r = 0.51) (Table 1) and the values fall in the field of normal marine limestones (Knauth and Kennedy, 2009) (Fig. 6) that suggests good preservation of the primary isotopic signal in this section. In the Tölgyhát section $\delta^{13}C$ and $\delta^{18}O$ data show a higher correlation in the Törökbükk Fm. (Pearson r = 0.6; Table 1) and also a larger variation in $\delta^{18}O$ and a much lower one in $\delta^{13}C$ (Fig. 6), suggesting a secondary diagenetic effect and a water-rock interaction with a limited amount of meteoric water, that generally has little impact on $\delta^{13}C$ (Lohmann, 1988). Diagenetic effect on the Úrkút Fm. appears more significant on the basis of $\delta^{13}C$-$\delta^{18}O$ correlation (Pearson r = 0.87; Table 1). Environmental changes related to the Jenkyns Event could lead to this strong correlation in the Úrkút Manganese Ore, however, such negative $\delta^{18}O$ data (> -7‰) suggests that the oxygen isotope composition was probably affected by later diagenetic overprint to some degree. Additionally, the most negative $\delta^{13}C$ values (~ -5 to -6‰) are lower than in published early Toarcian bulk carbonate records (Hesselbo et al., 2007; Bodin et al., 2016; Hermoso et al., 2009). Such low values are commonly related to organic matter remineralization and precipitation of ^{13}C-depleted carbonate in organic-rich mudstones, forming during early diagenesis under anaerobic conditions when sulphate reduction takes place (Wohlwend et al., 2016; Bodin et al., 2016; Arabas et al., 2017). Although this possibility cannot be excluded, the stratigraphic position (Fig. 3) and the facies characteristics suggest that the negative CIE in the Úrkút Manganese Ore Fm. at Tölgyhát represents the Jenkyns Event. Regional correlation provides further support as this formation is much thicker and particularly manganese-rich in the Bakony Mts. where it yielded organic carbon isotope values between -32 and -34 ‰ that is typical for the negative CIE (Polgári et al., 2016). In the higher part of the section, in the Kisgerecse Fm., a negative correlation between $\delta^{13}C$ and $\delta^{18}O$ (Pearson r = -0.5) and normal marine range of values (Fig. 6) suggests good preservation of the isotopic signal.

Calcareous nannofossils of the Tölgyhát section, where present, are poorly preserved with traces of overgrowth (Table 2). This suggests some secondary diagenetic precipitation of calcite during burial (Adelseck et al., 1973).

Trace elements in carbonate, primarily Mn and Sr and their ratios to Ca are also widely used as a tool for screening diagenetic alteration in carbonate sediments. Mn concentration increases whereas Sr decreases during dissolution and recrystallization of carbonates due to interaction with meteoric water (Brand et al., 2012a; 2012b; Schobben et al., 2016). In this case, however, Mn is not a reliable elemental indicator to use since the studied pelagic formations are particularly rich in Mn-oxides (Figs. 4 and 5) and it is generally present as dispersed microscopic to macroscopic nodules and coating on bio- and intraclasts, which was not possible to avoid during sampling. The Sr content, on the other hand, is not biased therefore the Sr/Ca ratio was additionally used for screening diagenetic overprint (Fig. 6). Neither $\delta^{13}C$ nor $\delta^{18}O$ shows a significant positive correlation with Sr/Ca in any of the samples from both sections and the different formations which further supports the good preservation of the isotopic signals (Table 1; Fig. 6).

In summary, the carbon isotope records from the Kisgerecse and Tölgyhát sections indicate good preservation of original environmental signals, whereas the oxygen isotope record is potentially altered by diagenesis to a certain degree therefore it is not suitable for paleoclimatic interpretation. However, $\delta^{13}C$ data from the Úrkút Manganese Ore Fm. might have been affected by organic matter remineralization to some extent.

Carbon isotope records and integrated stratigraphic correlation

Previously, Jenkyns & Clayton (1986) and Jenkyns et al. (1991) reported carbon isotope and stratigraphic information from two localities of the Gerecse Hills (Kisgerecse and Bánya-hegy) and investigated their relationship with other Tethyan localities. Here, we constructed high-resolution geochemical records and nannofossil biostratigraphy for the Tölgyhát and Kisgerecse sections in order to further explore the impact of the Jenkyns Event in the pelagic realm. A correlation between the two studied sections from the Gerecse Hills with the stratigraphically continuous and complete sedimentary record of the Peniche section from the Lusitanian Basin (Portugal) (Hesselbo et al., 2007; Rocha et al., 2016) has been carried out using the combination of biostratigraphical and high-resolution carbon isotope data (Fig. 8). The comprehensively studied Peniche section serves as the GSSP for the Toarcian Stage (Rocha et al., 2016) and as such, correlated with all other sections worldwide that record the Jenkyns event. The Pliensbachian part of the Törökbükk Limestone of the Tölgyhát and the Kisgerecse sections do not show any significant $\delta^{13}C$ trends. Its latest Pliensbachian age (Császár et al., 1998; Jenkyns et al., 1991) is also confirmed in the Tölgyhát section by the presence of the NJT5b nannofossil zone which spans the Pliensbachian/Toarcian boundary (Ferreira et al., 2019). Together with $\delta^{13}C$ data, this suggests that the deposition of this facies ended in the latest Pliensbachian before the Pliensbachian/Toarcian Event (Littler et al., 2010; Ait-Itto et al., 2017). The Pliensbachian carbon isotope data from Tölgyhát varies within a similar range compared to Peniche (approx. between 0–1‰), whereas at Kisgerecse the values are slightly higher, between 2–3‰ (Fig. 8). Considering the biostratigraphical uncertainties and the proximity to Tölgyhát this likely suggests that the $\delta^{13}C$ record at Kisgerecse does not include the uppermost Pliensbachian. Such positive values were reported from the Margaritatus Zone (Suan et al., 2010; Silva et al., 2011), however, the absence of precise biostratigraphic constraints preclude an unambiguous correlation. The

Pliensbachian/Toarcian Event is likely associated with the onset of greenhouse gas release from the Karoo-Ferrar LIP and it is characterised by a distinct negative CIE in the lowest part of the Polymorphum Zone or its equivalent, the Tenuicostatum Zone (Hesselbo et al., 2007; Littler et al., 2010; Ait-Itto et al., 2017) and the NJT5c nannofossil zone (Ferreira et al., 2019). This negative CIE is well-represented at Peniche (Hesselbo et al., 2007), but it is stratigraphically not documented in the Gerecse sections. The Pliensbachian/Toarcian Event is followed by a broad positive $\delta^{13}C$ excursion, likely related to enhanced organic production and carbon burial on a global scale in the Polymorphum (=Tenuicostatum) Zone preceding the pronounced negative CIE at the T-OAE (Hesselbo et al., 2007; Hermoso et al., 2012; Müller et al., 2020b). This positive excursion is also missing at both the Tölgyhát and Kisgerecse sections, only a highly condensed ~5 cm thick bed is assigned to the Tenuicostatum Zone (Géczy, 1984; 1985; Kovács, 2012) (Fig. 8). According to the astrochronological record reported by Suan et al. (2008b) and confirmed by Huang & Hesselbo (2014) for the Peniche section, a record of a ~800 kyr interval with the Pliesbachian/Toarcian Event and the subsequent positive excursion is missing from Tölgyhát but is at least partly present in Kisgerecse in the highly condensed Tenuicostatum Zone bed (Fig. 8). The hallmark of the Jenkyns Event is a sharp negative CIE of ~4-6‰ that commonly falls into the uppermost Tenuicostatum and the lower Serpentinum (≈Levisoni) Zones, that is globally recognized and is present in biogenic calcite, micrite and organic matter as well (Hesselbo et al., 2000; van Breugel et al., 2006; Hesselbo et al., 2007; Hermoso et al., 2009; Suan et al., 2010; Caruthers et al., 2011; Gröcke et al., 2011; Izumi et al., 2012; Al-Suwaidi et al., 2016; Bodin et al., 2016). This CIE is a useful tool for stratigraphic correlation of different sections. The T-OAE and negative CIE (associated with the Jenkyns Event) are well represented at Peniche with a duration of ~600-650 kyr (Suan et al., 2008b; Huang & Hesselbo, 2014) is only recorded in the Tölgyhát section in the Gerecse Hills, in the upper half of the Úrkút Fm. in a highly condensed ~24 cm interval covering the upper half of the yellow marl and the black shale layer (Fig. 8). The negative CIE is followed by another positive excursion (a rebound), with an approximate duration of ~480 kyr as determined in Peniche and at other localities (Huang & Hesselbo, 2014) where the sedimentation rate was fairly constant and the record continues in the upper Levisoni Zone (Hesselbo et al., 2007; Xu et al., 2018a; Suan et al., 2015; Ruebsam et al., 2020b) or upper NJT6a zone (Ferreira et al., 2019). This interval is at least partly recognised at both Tölgyhát and Kisgerecse (Fig. 8).

Impact of environmental change on pelagic carbonate systems

Multiple studies have suggested a calcification crisis that spans the Jenkyns Event (Mattioli et al., 2009; Trecalli et al., 2012; Ettinger et al., 2021), although brachiopod shell-based δ^{11}B-pH data and a carbonate saturation model imply that the development of triggering factors commenced earlier, already at the Pliensbachian/Toarcian Event (Krencker et al., 2020; Müller et al., 2020a). Shallow-water carbonate platforms, carbonate production in epicontinental basins and hemipelagic-pelagic settings open to the Tethys Ocean were all severely affected (Mattioli et al., 2009; Trecalli et al., 2012; Suan et al., 2018; Müller et al., 2020b). Several mechanisms have been postulated for interpreting this calcification crisis. First, increasing global seawater temperature and associated acceleration of hydrological cycle and eutrophication of the water column (Suan et al., 2008a) or, alternatively, thermohaline stratification of surface waters triggered a decrease in nutrient levels of surface waters, adversely affecting the calcareous phytoplankton (Mattioli et al., 2009). Second, a eustatic sea-level rise may have resulted in the drowning of carbonate platforms and, as a consequence, also in carbonate shortage in epicontinental basinal settings (Bodin et al., 2010; Léonide et al., 2012; Pittet et al., 2014), which could also explain the carbonate shortage in hemipelagic-pelagic ocean-facing basins (Müller et al., 2020b). Third, ocean acidification could have developed due to the input of excess CO_2 into the ocean-atmosphere system, lowering both the seawater pH and calcite saturation level ($\Omega<1$) (Trecalli et al., 2012; Ettinger et al., 2021; Müller et al., 2020a). Fourth, enhanced continental weathering and an increase in siliciclastic supply may have led to carbonate factory shutdown in shallow-water carbonate platforms (Krencker et al., 2020).

The results of chemostratigraphic correlation in combination with biostratigraphy of the continuous and complete Peniche section with Tölgyhát and Kisgerecse (Fig. 8) indicates significant condensation and hiatuses at certain levels of these pelagic carbonate successions in the western Tethys. The temporal coincidence of these sedimentary features with the Pliensbachian/Toarcian Event and the Jenkyns Event suggests that global warming and concomitant calcification crises substantially affected the pelagic carbonate systems in the Gerecse. A major hiatus in these lower Toarcian sections occurs in the Tenuicostatum Zone, which is commonly associated with hardgrounds on the top of the upper Pliensbachian Törökbükk Fm. (Császár et al., 1998; Kovács, 2012). The absence of the Tenuicostatum Zone, with the exception of the Kisgerecse section, and the sudden drop of $CaCO_3$ from ~80 to 3 wt% simultaneously with the negative CIE in the Tölgyhát section suggests that adverse environmental conditions leading to the shutdown of pelagic carbonate production developed in the Gerecse basin already around the Pliensbachian/Toarcian Event and persisted during the Jenkyns Event. Elsewhere, brachiopod boron isotope-based pH reconstruction, carbonate saturation state models, and sedimentological evidence from shallow marine carbonate platforms previously supported that low pH conditions indeed started to develop at the Pliensbachian/Toarcian Event and seawater pH fluctuated reaching its minimum immediately prior to and during the Jenkyns Event (Müller et al., 2020a; Ettinger et al., 2021). Hardgrounds and gaps are often associated with the Pliensbachian/Toarcian boundary and the lower Toarcian at other Tethyan localities as well (e.g. Léonide et al., 2013; Pittet et al., 2014; Arabas et al., 2017; Rosales et al., 2018; Fantasia et al., 2018). The appearance of hardgrounds at the same stratigraphic level in the Adriatic Carbonate Platform has been explained by submarine dissolution due to shoaling of CCD as a consequence of CO_2-rich, undersaturated bottom waters as a result of massive CO_2 input into the ocean-atmosphere system from the Karoo-Ferrar LIP (Ettinger et al., 2021). This scenario could be potentially also applicable for pelagic carbonate successions such as these at Tölgyhát and Kisgerecse. Additionally, the marine transgression associated with the Jenkyns Event (Haq, 2018; Ruebsam et al., 2019) likely played a role in the drowning of nearby platforms (Léonide et al., 2013) thereby reducing carbonate sediment supply into the basins and also moving the source of detrital input farther away. Taken together, these factors arrested the carbonate sedimentation and resulted in a condensed record of the Jenkyns Event and contemporaneous gaps in the pelagic successions of the Gerecse basin. Mineralogical composition of detrital components of the Tölgyhát section indicates high illite and quartz content for the Úrkút Fm., but negligible kaolinite, randomly interstratified illite/smectite and microcline (Fig. 7). Kaolinite is often present in abundance in NW European sections where it has been considered as an indicator for intense continental weathering with high water-rock ratio, due to the global warming and accelerated hydrological cycle during the Jenkyns Event (Raucsik & Varga, 2008; Dera et al., 2009). The low kaolinite content in the Úrkút Fm. at Tölgyhát suggests a very distal position of the Gerecse basin, similar to the observations from the Lombardian Basin (Fantasia et al., 2018)

Conclusions

In this study, we present new high-resolution geochemical data from two upper Pliensbachian – lower Toarcian pelagic sections from the Gerecse Hills (Hungary), Tölgyhát and Kisgerecse, complemented with new nannofossil biostratigraphic data from Tölgyhát. The deposition of the pelagic successions that consist of limestone, marl and black shale in these sections took place in proximity to the open Tethys Ocean near its northwestern shelf. The carbon isotope record of the Tölgyhát section shows that the negative CIE related to the Jenkyns Event is only present in a 24 cm thick highly condensed black shale layer, where bulk calcium carbonate and calcite content drop significantly from ~80 to 3 wt%. In the Kisgerecse section, this isotope anomaly is not recorded due to a stratigraphic gap. The stratigraphic position of gaps, condensation and hardgrounds in these successions coincides with the Pliensbachian/Toarcian Event and the Jenkyns Event, suggesting that the pelagic carbonate system was severely affected by calcification crises, likely due to large scale CO_2 emission coincident with these events. Additionally, a sea-level rise during the Jenkyns Event could significantly decrease carbonate and siliclastic material input, facilitating sedimentary condensation and the development of hiatuses. Our results add to a growing body of evidence that perturbations of the Jenkyns Event were global in extent and severely affected different sedimentary environments, including pelagic carbonate depositional systems.

Acknowledgments

Help in sampling in the field was provided by Mariann Bosnakoff, Dóra Kesjár, and Zoltán Szentesi. László Fodor, Orsolya Sztanó, and students of Eötvös Loránd University's geology field school are thanked for their inspiration and discussions about the geology of Gerecse Hills. Constructive reviews of Stéphane Bodin and Andrew Caruthers and additional suggestions of editor Luís Vítor Duarte helped to improve the manuscript significantly. This study received funding by the National Research, Development and Innovation Office of Hungary (Grants OTKA NN 128702 and K 135309). The research was also supported by the European Union and the State of Hungary, co-financed by the European Regional Development Fund in the project of GINOP-2.3.2.-15-2016- 00009 'ICER'. This is a contribution to IGCP Project 655 and MTA-MTM-ELTE Paleo contribution No. 345.

References

Adelseck, C.G., Geehan, G.W. and Roth, P.H. 1973. Experimental evidence for the selective dissolution and overgrowth of calcareous nannofossils during diagenesis. *Geological Society of America Bulletin*, **84**, 2755–2762, https://doi.org/10.1130/0016-7606(1973)84%3C2755:eeftsd%3E2.0.co;2

Ait-Itto, F.Z., Price, G.D., Addi, A.A., Chafiki, D. and Mannani, I. 2017. Bulk-carbonate and belemnite carbon-isotope records across the Pliensbachian-Toarcian boundary on the northern margin of Gondwana (Issouka, Middle Atlas, Morocco). *Palaeogeography, Palaeoclimatology, Palaeoecology*, **466**, 128-136, https://doi.org/10.1016/j.palaeo.2016.11.014

Al-Suwaidi, A.H., Hesselbo, S.P., Damborenea, S.E., Manceñido, M.O., Jenkyns, H.C., Riccardi, A.C., Angelozzi, G.N. and Baudin, F. 2016. The Toarcian Oceanic Anoxic Event (Early Jurassic) in the Neuquén Basin, Argentina: a reassessment of age and carbon isotope stratigraphy. *The Journal of Geology*, **124**, 171-193, https://doi.org/10.1086/684831
Arabas, A., Schlögl, J. and Meister, C. 2017. Early Jurassic carbon and oxygen isotope records and seawater temperature variations: Insights from marine carbonate and belemnite rostra (Pieniny Klippen Belt, Carpathians). *Palaeogeography, Palaeoclimatology, Palaeoecology*, **485**, 119-135, https://doi.org/10.1016/j.palaeo.2017.06.007
Bailey, T.R., Rosenthal, Y., McArthur, J.M., van de Schootbrugge, B. and Thirlwall, M.F. 2003. Paleoceanographic changes of the Late Pliensbachian–Early Toarcian interval: a possible link to the genesis of an Oceanic Anoxic Event. *Earth and Planetary Science Letters*, **212**, 307-320, https://doi.org/10.1016/s0012-821x(03)00278-4
Bish, D.L. and Post, J.E., 1993. Quantitative mineralogical analysis using the Rietveld full-pattern fitting method. *American Mineralogist*, **78**, 932-940.
Bodin, S., Mattioli, E., Fröhlich, S., Marshall, J.D., Boutib, L., Lahsini, S. and Redfern, J. 2010. Toarcian carbon isotope shifts and nutrient changes from the Northern margin of Gondwana (High Atlas, Morocco, Jurassic): palaeoenvironmental implications. *Palaeogeography, Palaeoclimatology, Palaeoecology*, **297**, 377-390, https://doi.org/10.1016/j.palaeo.2010.08.018
Bodin, S., Krencker, F.N., Kothe, T., Hoffmann, R., Mattioli, E., Heimhofer, U. and Kabiri, L. 2016. Perturbation of the carbon cycle during the late Pliensbachian–early Toarcian: New insight from high-resolution carbon isotope records in Morocco. *Journal of African Earth Sciences*, *116*, 89-104, http://.doi.org/10.1016/j.jafrearsci.2015.12.018
Bown, P.R. and Cooper, M.K.E. 1998. Calcareous nannofossils biostratigraphy. In: P.R. Bown (Ed.), *Calcareous Nannoplankton Biostratigraphy*, British Micropaleontological Press, 34-85.
Bown, P.R., Young, J.R. 1998. Techniques. In: P.R. Bown (Ed.), *Calcareous Nannoplankton Biostratigraphy*, British Micropaleontological Press, 16-28.
Brand, U. and Veizer, J. 1981. Chemical diagenesis of a multicomponent carbonate system; 2, Stable isotopes. *Journal of Sedimentary Research*, **51**, 987-997, https://doi.org/10.1306/212f7df6-2b24-11d7-8648000102c1865d
Brand, U., Jiang, G., Azmy, K., Bishop, J., Montanez, I.P. 2012a. Diagenetic evaluation of a Pennsylvanian carbonate succession (Bird Spring Formation, Arrow Canyon, Nevada, USA)-1: Brachiopod and whole rock comparison. *Chemical Geology*, **308**, 26–39, https://doi.org/10.1016/j.chemgeo.2012.03.017
Brand, U., Posenato, R., Came, R., Affek, H., Angiolini, L., Azmy, K., Farabegoli, E. 2012b. The end-Permian mass extinction: a rapid volcanic CO_2 and CH_4-climatic catastrophe. *Chemical Geology*, **322**, 121–144, https://doi.org/10.1016/j.chemgeo.2012.06.015
Brunton, G. 1955. Vapour pressure glycolation of oriented clay minerals. *American Mineralogist*, **40**, 124–126.
Budai, T., Fodor, L., Sztanó, O., Kercsmár, Z., Császár, G., Csillag, G., Gál, N., Kele, S., Kiszely, M., Selmeczi, I., Babinszki, E., Thamóné Bozsó, E., and Lantos, Z. 2018, A Gerecse hegység földtana. Magyarázó a Gerecse hegység földtani térképéhez (1:50 000). (Geology of the Gerecse Mountains. Explanatory book to the geological map of the Gerecse Mountains (1:50 000)), Budapest, Magyar Bányászati és Földtani Szolgálat (Hungarian Mining and Geological Survey), Magyarország tájegységi térképsorozata (Regional map series of Hungary), 490 p.
Bucefalo Palliani, R., Mattioli, E., Riding, J. 2002. The response of marine phytoplankton and sedimentary organic matter to the early Toarcian (Lower Jurassic) oceanic anoxic event

in northern England. *Marine Micropaleontology*, **46**, 223-245, https://doi.org/10.1016/s0377-8398(02)00064-6
Caruthers, A.H., Gröcke, D.R. and Smith, P.L. 2011. The significance of an Early Jurassic (Toarcian) carbon-isotope excursion in Haida Gwaii (Queen Charlotte Islands), British Columbia, Canada. *Earth and Planetary Science Letters*, **307**, 19-26, https://doi.org/10.1016/j.epsl.2011.04.013
Caruthers, A.H., Smith, P.L. and Gröcke, D.R. 2014. The Pliensbachian–Toarcian (Early Jurassic) extinction: a North American perspective. *Geological Society of America Special Papers*, **505**, 225-243 https://doi.org/10.1130/2014.2505(11)
Caswell, B.A., Coe, A.L. and Cohen, A.S. 2009. New range data for marine invertebrate species across the early Toarcian (Early Jurassic) mass extinction. *Journal of the Geological Society*, **166**, 859-872, https://doi.org/10.1144/0016-76492008-0831
Cohen, A.S., Coe, A.L., Harding, S.M. and Schwark, L. 2004. Osmium isotope evidence for the regulation of atmospheric CO2 by continental weathering. *Geology*, **32**, 157-160, https://doi.org/10.1130/g20158.1
Császár, G., Galácz, A. and Vörös, A. 1998. A gerecsei jura — fácieskérdések, alpi analógiák. [Jurassic of the Gerecse Mountains, Hungary: facies and Alpine analogies] *Földtani Közlöny*, **128**, 397-435.
Danise, S., Twitchett, R.J., Little, C.T. and Clémence, M.E. 2013. The impact of global warming and anoxia on marine benthic community dynamics: an example from the Toarcian (Early Jurassic). *PLoS One*, **8**, p.e56255, https://doi.org/10.1371/journal.pone.0056255
Dera, G., Pellenard, P., Neige, P., Deconinck, J. F., Pucéat, E. and Dommergues, J. L. 2009. Distribution of clay minerals in Early Jurassic Peritethyan seas: palaeoclimatic significance inferred from multiproxy comparisons. *Palaeogeography, Palaeoclimatology, Palaeoecology*, **271**, 39-51, https://doi.org/10.1016/j.palaeo.2008.09.010
Dulai, A. 1998. Early Jurassic brachiopods from the basal layers of the Pisznice Limestone of Lábatlan (Gerecse Mts, Hungary). *Annales historico-naturales Musei nationalis hungarici*, **90**, 35-55.
Ettinger, N.P., Larson, T.E., Kerans, C., Thibodeau, A.M., Hattori, K.E., Kacur, S.M. and Martindale, R.C. 2021. Ocean acidification and photic-zone anoxia at the Toarcian Oceanic Anoxic Event: Insights from the Adriatic Carbonate Platform. *Sedimentology*, **68**, 63-107, https://doi.org/10.1111/sed.12786
Fantasia, A., Föllmi, K.B., Adatte, T., Spangenberg, J.E. and Montero-Serrano, J.C. 2018. The Early Toarcian oceanic anoxic event: Paleoenvironmental and paleoclimatic change across the Alpine Tethys (Switzerland). *Global and Planetary Change*, **162**, 53-68, https://doi.org/10.1016/j.gloplacha.2018.01.008
Ferreira, J., Mattioli, E., Suchéras-Marx, B., Giraud, F., Duarte, L.V., Pittet, B., Suan, G., Hassler, A. and Spangenberg, J.E. 2019. Western Tethys Early and Middle Jurassic calcareous nannofossil biostratigraphy. *Earth-Science Reviews*, **197**, 102908, https://doi.org/10.1016/j.earscirev.2019.102908
Főzy, I. (Ed.) 2012. *Magyarország litosztratigráfiai alapegységei. Jura* [*Lithostratigraphic Units of Hungary. Jurassic*]. Hungarian Geological Society, Budapest, 235 pp.
Fülöp, J. 1976. The Mesozoic basement horst blocks of Tata. *Geologica Hungarica, series Geologica*, **16**, 1-228.
Galácz, A., Császár, G., Géczy, B. and Kovács, Z. 2010. Ammonite stratigraphy of a Toarcian (Lower Jurassic) section on Nagy-Pisznice Hill (Gerecse Mts, Hungary). *Central European Geology*, **53**, 311-342.
Géczy, B. 1984: Provincialism of Jurassic ammonites, examples from Hungarian faunas. – *Acta Geologica Hungarica*, **27**, 379–389.

Géczy, B. 1985: Toarci Amonites zónák a Gerecse hegységben. *Földtani Közlöny*, **115**, 363-368.
Gröcke, D.R., Hori, R.S., Trabucho-Alexandre, J., Kemp, D.B. and Schwark, L. 2011. An open ocean record of the Toarcian oceanic anoxic event. *Solid Earth*, **2**, 245-257, https://doi.org/10.5194/se-2-245-2011
Haas, J. 2012. Influence of global, regional, and local factors on the genesis of the Jurassic manganese ore formation in the Transdanubian Range, Hungary. *Ore Geology Reviews*, **47**, 77-86, https://doi.org/10.1016/j.oregeorev.2011.08.006
Haq, B.U. 2018. Jurassic sea-level variations: a reappraisal. *GSA Today*, **28**, 4-10. https://doi.org/https://doi.org/10.1130/GSATG359A.1
Häusler, H., Plašienka, D. and Polák, M. 1993. Comparison of Mesozoic successions in the Central Eastern Alps and the Central Western Carpathians. *Jahrbuch der Geologischen Bundesanstalt*, **136**, 715–739.
Hermoso, M., Le Callonnec, L., Minoletti, F., Renard, M. and Hesselbo, S.P. 2009. Expression of the Early Toarcian negative carbon-isotope excursion in separated carbonate microfractions (Jurassic, Paris Basin). *Earth and Planetary Science Letters*, **277**, 194-203, https://doi.org/10.1016/j.epsl.2008.10.013
Hermoso, M., Minoletti, F., Rickaby, R.E., Hesselbo, S.P., Baudin, F. and Jenkyns, H.C. 2012. Dynamics of a stepped carbon-isotope excursion: Ultra high-resolution study of Early Toarcian environmental change. *Earth and Planetary Science Letters*, **319**, 45-54, https://doi.org/10.1016/j.epsl.2011.12.021
Hesselbo, S.P. and Pieńkowski, G. 2011. Stepwise atmospheric carbon-isotope excursion during the Toarcian oceanic anoxic event (Early Jurassic, Polish Basin). *Earth and Planetary Science Letters*, **301**, 365-372, https://doi.org/10.1016/j.epsl.2010.11.021
Hesselbo, S.P., Gröcke, D.R., Jenkyns, H.C., Bjerrum, C.J., Farrimond, P., Bell, H.S.M. and Green, O.R. 2000. Massive dissociation of gas hydrate during a Jurassic oceanic anoxic event. *Nature*, **406**, 392-395, https://doi.org/10.1038/35019044
Hesselbo, S.P., Jenkyns, H.C., Duarte, L.V. and Oliveira, L.C. 2007. Carbon-isotope record of the Early Jurassic (Toarcian) Oceanic Anoxic Event from fossil wood and marine carbonate (Lusitanian Basin, Portugal). *Earth and Planetary Science Letters*, **253**, 455-470, https://doi.org/10.1016/j.epsl.2006.11.009
Huang, C. and Hesselbo, S.P. 2014. Pacing of the Toarcian Oceanic Anoxic Event (Early Jurassic) from astronomical correlation of marine sections. *Gondwana Research*, **25**, 1348-1356, https://doi.org/10.1016/j.gr.2013.06.023
Izumi, K., Miyaji, T. and Tanabe, K. 2012. Early Toarcian (Early Jurassic) oceanic anoxic event recorded in the shelf deposits in the northwestern Panthalassa: Evidence from the Nishinakayama Formation in the Toyora area, west Japan. *Palaeogeography, Palaeoclimatology, Palaeoecology*, **315**, 100-108, https://doi.org/10.1016/j.palaeo.2011.11.016
Jenkyns, H.C. 1988. The early Toarcian (Jurassic) anoxic event-stratigraphic, sedimentary, and geochemical evidence. *American Journal of Science*, **288**, 101-151, https://doi.org/10.2475/ajs.288.2.101
Jenkyns, H.C. 2010. Geochemistry of oceanic anoxic events. *Geochemistry, Geophysics, Geosystems*, **11**, 1-30
Jenkyns, H.C. and Clayton, C.J. 1986. Black shales and carbon isotopes in pelagic sediments from the Tethyan Lower Jurassic. *Sedimentology*, **33**, 87-106, https://doi.org/10.1111/j.1365-3091.1986.tb00746.x
Jenkyns, H.C., Géczy, B. and Marshall, J.D. 1991. Jurassic manganese carbonates of central Europe and the early Toarcian anoxic event. *The Journal of Geology*, **99**, 137-149, https://doi.org/10.1086/629481

Kafousia, N., Karakitsios, V., Jenkyns, H.C. and Mattioli, E. 2011. A global event with a regional character: the Early Toarcian Oceanic Anoxic Event in the Pindos Ocean (northern Peloponnese, Greece). *Geological Magazine*, **148**, 619-631, https://doi.org/10.1017/s0016756811000082
Kemp, D.B., Coe, A.L., Cohen, A.S. and Schwark, L. 2005. Astronomical pacing of methane release in the Early Jurassic period. *Nature*, **437**, 396-399, https://doi.org/10.1038/nature04037
Kemp, D.B., Selby, D. and Izumi, K. 2020. Direct coupling between carbon release and weathering during the Toarcian oceanic anoxic event. *Geology*, **48**, 976-980, https://doi.org/10.1130/g47509.1
Knauth, L.P. and Kennedy, M.J. 2009. The late Precambrian greening of the Earth. *Nature*, **460**, 728-732, https://doi.org/10.1038/nature08213
Konda, J. 1986. Gerecse, Süttő, Kisgerecsei kőfejtő (Kisgerecse quarry, Süttő, Gerecse), Magyar Állami Földtani Intézet (Hungarian Geological Institute), Magyarország geológiai alapszelvényei [Geological Reference Sections of Hungary], 8 p.
Konda, J. 1988. Gerecse, Lábatlan, Tölgyháti kőfejtő (Tölgyhát quarry, Lábatlan, Gerecse), Magyar Állami Földtani Intézet (Hungarian Geological Institute), Magyarország geológiai alapszelvényei [Geological Reference Sections of Hungary], 8 p.
Kovács, Z. 2012. Lower Toarcian Ammonitida fauna and biostratigraphy of the Gerecse Mountains (Hungary). *Fragmenta Palaeontologica Hungarica*, **29**, 1-48.
Krencker, F.N., Lindström, S. and Bodin, S. 2019. A major sea-level drop briefly precedes the Toarcian oceanic anoxic event: implication for Early Jurassic climate and carbon cycle. *Scientific Reports*, **9**, 12518, https://doi.org/10.1038/s41598-019-48956-x
Krencker, F.N., Fantasia, A., Danisch, J., Martindale, R., Kabiri, L., El Ouali, M. and Bodin, S. 2020. Two-phased collapse of the shallow-water carbonate factory during the late Pliensbachian–Toarcian driven by changing climate and enhanced continental weathering in the Northwestern Gondwana Margin. *Earth-Science Reviews*, **208**, 103254, https://doi.org/10.1016/j.earscirev.2020.103254
Küspert, W. 1982. Environmental changes during oil shale deposition as deduced from stable isotope ratios. *In:* Einsele, G. and Seilacher, A. (eds) *Cyclic and Event Stratification.* Springer, 482-501, https://doi.org/10.1007/978-3-642-75829-4_36
Léonide, P., Floquet, M., Durlet, C., Baudin, F., Pittet, B. and Lécuyer, C. 2012. Drowning of a carbonate platform as a precursor stage of the Early Toarcian global anoxic event (Southern Provence sub-Basin, South-east France). *Sedimentology*, *59*, 156-184, https://doi.org/10.1111/j.1365-3091.2010.01221.x
Littler, K., Hesselbo, S.P. and Jenkyns, H.C. 2010. A carbon-isotope perturbation at the Pliensbachian–Toarcian boundary: evidence from the Lias Group, NE England. *Geological Magazine*, **147**, 181-192, https://doi.org/10.1017/s0016756809990458
Lohmann, K.C. 1988. Geochemical patterns of meteoric diagenetic systems and their application to studies of paleokarst. *In*: James N.P. and Choquette P.W. (eds) *Paleokarst*. Springer, 58-80, https://doi.org/10.1007/978-1-4612-3748-8_3
Marquart, R.G.,Katsnelson, I., Milne, G.W.A., Heller, S.R., Johnson, G.G., Jenkyns, R. 1979. A search-match system for X-ray powder diffraction data. *Journal of Applied Crystallography*, **12**, 629-634.
Mattioli, E., Erba, E. 1999. Biostratigraphic synthesis of calcareous nannofossil events in the Tethyan Jurassic. *Rivista Italiana di Paleontologia e Stratigrafia* 105, 343-376.
Mattioli, E., Pittet, B., Petitpierre, L. and Mailliot, S. 2009. Dramatic decrease of pelagic carbonate production by nannoplankton across the Early Toarcian anoxic event (T-OAE). *Global and Planetary Change*, **65**, 134-145, https://doi.org/10.1016/j.gloplacha.2008.10.018

McElwain, J.C., Wade-Murphy, J. and Hesselbo, S.P. 2005. Changes in carbon dioxide during an oceanic anoxic event linked to intrusion into Gondwana coals. *Nature*, **435**, 479-482, https://doi.org/10.1038/nature03618
Meister, C., Schirolli, P. and Dommergues, J.-L. 2017. Early Jurassic (Sinemurian to basal Toarcian) ammonites of the Brescian Prealps (Southern Alps, Italy). *Rivista Italiana di Paleontologia e Stratigrafia*, **123**, 79-148, https://doi.org/10.13130/2039-4942/8072
Müller, T., Price, G.D., Bajnai, D., Nyerges, A., Kesjár, D., Raucsik, B., Varga, A., Judik, K., Fekete, J., May, Z. and Pálfy, J. 2017. New multiproxy record of the Jenkyns Event (also known as the Toarcian Oceanic Anoxic Event) from the Mecsek Mountains (Hungary): Differences, duration and drivers. *Sedimentology*, **64**, 66-86, https://doi.org/10.1111/sed.12332
Müller, T., Jurikova, H., Gutjahr, M., Tomašových, A., Schlögl, J., Liebetrau, V., Duarte, L.V., Milovský, R., Suan, G., Mattioli, E. and Pittet, B. 2020a. Ocean acidification during the early Toarcian extinction event: Evidence from boron isotopes in brachiopods. *Geology*, **48**, 1184-1188, https://doi.org/10.1130/G47781.1
Müller, T., Karancz, S., Mattioli, E., Milovský, R., Pálfy, J., Schlögl, J., Segit, T., Šimo, V. and Tomašových, A. 2020b. Assessing anoxia, recovery and carbonate production setback in a hemipelagic Tethyan basin during the Toarcian Oceanic Anoxic Event (Western Carpathians). *Global and Planetary Change*, **195**, 103366, https://doi.org/10.1016/j.gloplacha.2020.103366
Neumeister, S., Gratzer, R., Algeo, T.J., Bechtel, A., Gawlick, H.J., Newton, R.J. and Sachsenhofer, R.F. 2015. Oceanic response to Pliensbachian and Toarcian magmatic events: Implications from an organic-rich basinal succession in the NW Tethys. *Global and Planetary Change*, **126**, 62-83, https://doi.org/10.1016/j.gloplacha.2015.01.007
Pálfy, J. and Smith, P.L. 2000. Synchrony between Early Jurassic extinction, oceanic anoxic event, and the Karoo-Ferrar flood basalt volcanism. *Geology*, **28**, 747-750, https://doi.org/10.1130/0091-7613(2000)028%3C0747:sbejeo%3E2.3.co;2
Pearce, C.R., Cohen, A.S., Coe, A.L. and Burton, K.W. 2008. Molybdenum isotope evidence for global ocean anoxia coupled with perturbations to the carbon cycle during the Early Jurassic. *Geology*, **36**, 231-234, https://doi.org/10.1130/g24446a.1
Percival, L.M., Cohen, A.S., Davies, M.K., Dickson, A.J., Hesselbo, S.P., Jenkyns, H.C., Leng, M.J., Mather, T.A., Storm, M.S. and Xu, W. 2016. Osmium isotope evidence for two pulses of increased continental weathering linked to Early Jurassic volcanism and climate change. *Geology*, **44**, 759-762, https://doi.org/10.1130/g37997.1
Pittet, B., Suan, G., Lenoir, F., Duarte, L.V., Mattioli, E. 2014. Carbon isotope evidence for sedimentary discontinuities in the lower Toarcian of the Lusitanian Basin (Portugal): sea level changes at the onset of the Oceanic Anoxic Event. *Sedimentary Geology* 303, 1-14.
Polgári, M., Szabó, Z. and Szederkényi, T. (eds) 2000. *Mangánércek Magyarországon – Grasselly Gyula akadémikus emlékére* [*Manganese Ores in Hungary – Tribute to Professor Gyula Grasselly*]. Juhász Nyomda, 675 p. (in Hungarian)
Polgári, M., Hein, J.R., Bíró, L., Gyollai, I., Németh, T., Sajgó, C., Fekete, J., Schwark, L., Pál-Molnár, E., Hámor-Vidó, M. and Vigh, T. 2016. Mineral and chemostratigraphy of a Toarcian black shale hosting Mn-carbonate microbialites (Úrkút, Hungary). *Palaeogeography, Palaeoclimatology, Palaeoecology*, **459**, 99-120, https://doi.org/10.1016/j.palaeo.2016.06.030
Raucsik, B. and Varga, A. 2008. Climato-environmental controls on clay mineralogy of the Hettangian–Bajocian successions of the Mecsek Mountains, Hungary: an evidence for extreme continental weathering during the early Toarcian oceanic anoxic event. *Palaeogeography, Palaeoclimatology, Palaeoecology*, **265**, 1-13, https://doi.org/10.1016/j.palaeo.2008.02.004

Reolid, M., Mattioli, E., Duarte, L. and Marok, A. 2020. The Toarcian Oceanic Anoxic Event and the Jenkyns Event (IGCP-655 final report). *Episodes*, **43**, 833-844, https://doi.org/10.18814/epiiugs/2020/020051

Rocha, R.B., Mattioli, E., Duarte, L.V., Pittet, B., Elmi, S., Mouterde, R., Cabral, M.C., Comas-Rengifo, M.J., Gómez, J.J., Goy,A., Hesselbo, S.P., Jenkyns, H.C., Littler, K., Mailliot, S., Veiga de Oliveira, C., Osete, M.L., Perilli, N., Pinto, S., Ruget, C., Suan, G. 2016. Base of the Toarcian Stage of the Lower Jurassic defined by the Global Boundary Stratotype Section and Point (GSSP) at the Peniche section (Portugal). *Episodes*, **39**, 460-481, https://doi.org/10.18814/epiiugs/2016/v39i3/99741

Rosales, I., Quesada, S. and Robles, S. 2001. Primary and diagenetic isotopic signals in fossils and hemipelagic carbonates: the Lower Jurassic of northern Spain. *Sedimentology*, **48**, 1149-1169, https://doi.org/10.1046/j.1365-3091.2001.00412.x

Rosales, I., Barnolas, A., Goy, A., Sevillano, A., Armendáriz, M. and López-García, J.M. 2018. Isotope records (CO-Sr) of late Pliensbachian-early Toarcian environmental perturbations in the westernmost Tethys (Majorca Island, Spain). *Palaeogeography, Palaeoclimatology, Palaeoecology*, **497**, 168-185, https://doi.org/10.1016/j.palaeo.2018.02.016

Ruebsam, W., Müller, T., Kovács, J., Pálfy, J. and Schwark, L. 2018. Environmental response to the early Toarcian carbon cycle and climate perturbations in the northeastern part of the West Tethys shelf. *Gondwana Research*, **59**, 144-158, https://doi.org/10.1016/j.gr.2018.03.013

Ruebsam, W., Mayer, B., Schwark, L. 2019. Cryosphere carbon dynamics control early Toarcian global warming and sea level evolution. *Global and Planetary Change*, **172**, 440–453, https://doi.org/10.1016/j.gloplacha.2018.11.003

Ruebsam, W. and Al-Husseini, M. 2020b. Calibrating the Early Toarcian (Early Jurassic) with stratigraphic black holes (SBH). *Gondwana Research*, 82, 317-336, https://doi.org/10.1016/j.gr.2020.01.011

Sasvári, Á., Csontos, L. and Palotai, M. 2009: Szerkezetgeológiai megfigyelések a gerecsei Tölgyháti-kőfejtőben (Structural geological observations in Tölgyhát Quarry (Gerece Mts., Hungary). *Földtani Közlöny*, **139**, 55-66.

Schobben, M., Ullmann, C.V., Leda, L., Korn, D., Struck, U., Reimold, W.U., Ghaderi, A., Algeo, T.J. and Korte, C. 2016. Discerning primary versus diagenetic signals in carbonate carbon and oxygen isotope records: An example from the Permian–Triassic boundary of Iran. *Chemical Geology*, **422**, 94-107, https://doi.org/10.1016/j.chemgeo.2015.12.013

Schouten, S., van Kaam-Peters, H.M., Rijpstra, W.I.C., Schoell, M. and Damste, J.S.S. 2000. Effects of an oceanic anoxic event on the stable carbon isotopic composition of early Toarcian carbon. *American Journal of Science*, **300**, 1-22, https://doi.org/10.2475/ajs.300.1.1

Silva, R.L., Duarte, L.V., Comas-Rengifo, M.J., Mendonça Filho, J.G. and Azerêdo, A.C. 2011. Update of the carbon and oxygen isotopic records of the Early–Late Pliensbachian (Early Jurassic,~ 187 Ma): Insights from the organic-rich hemipelagic series of the Lusitanian Basin (Portugal). *Chemical Geology*, **283**, 177-184, https://doi.org/10.1016/j.chemgeo.2011.01.010

Suan, G., Mattioli, E., Pittet, B., Mailliot, S. and Lécuyer, C. 2008a. Evidence for major environmental perturbation prior to and during the Toarcian (Early Jurassic) oceanic anoxic event from the Lusitanian Basin, Portugal. *Paleoceanography*, **23**, 1-14, https://doi.org/10.1029/2007pa001459

Suan, G., Pittet, B., Bour, I., Mattioli, E., Duarte, L.V. 2008b. Duration of the Early Toarcian carbon isotope excursion deduced from spectral analysis: consequence for its possible causes. *Earth and Planetary Science Letters*, **267**, 666-679, https://doi.org/10.1016/j.epsl.2007.12.017

Suan, G., Mattioli, E., Pittet, B., Lécuyer, C., Suchéras-Marx, B., Duarte, L.V., Philippe, M., Reggiani, L. and Martineau, F. 2010. Secular environmental precursors to Early Toarcian (Jurassic) extreme climate changes. *Earth and Planetary Science Letters*, **290**, 448-458, https://doi.org/10.1016/j.epsl.2009.12.047
Suan, G., Nikitenko, B.L., Rogov, M.A., Baudin, F., Spangenberg, J.E., Knyazev, V.G., Glinskikh, L.A., Goryacheva, A.A., Adatte, T., Riding, J.B. and Föllmi, K.B. 2011. Polar record of Early Jurassic massive carbon injection. *Earth and Planetary Science Letters*, **312**, 102-113, https://doi.org/10.1016/j.epsl.2011.09.050
Suan, G., van de Schootbrugge, B., Adatte, T., Fiebig, J. and Oschmann, W. 2015. Calibrating the magnitude of the Toarcian carbon cycle perturbation. *Paleoceanography*, **30**, 495-509, https://doi.org/10.1002/2014PA002758
Suan, G., Schlögl, J. and Mattioli, E. 2016. Bio-and chemostratigraphy of the Toarcian organic-rich deposits of some key successions of the Alpine Tethys. *Newsletters on Stratigraphy*, **49**, 401-419, https://doi.org/10.1127/nos/2016/0078
Suan, G., Schöllhorn, I., Schlögl, J., Segit, T., Mattioli, E., Lécuyer, C. and Fourel, F. 2018. Euxinic conditions and high sulfur burial near the European shelf margin (Pieniny Klippen Belt, Slovakia) during the Toarcian oceanic anoxic event. *Global and Planetary Change*, **170**, 246-259, https://doi.org/10.1016/j.gloplacha.2018.09.003
Svensen, H., Planke, S., Chevallier, L., Malthe-Sørenssen, A., Corfu, F. and Jamtveit, B. 2007. Hydrothermal venting of greenhouse gases triggering Early Jurassic global warming. *Earth and Planetary Science Letters*, **256**, 554-566, https://doi.org/10.1016/j.epsl.2007.02.013
Them II, T.R., Gill, B.C., Caruthers, A.H., Gröcke, D.R., Tulsky, E.T., Martindale, R.C., Poulton, T.P. and Smith, P.L. 2017. High-resolution carbon isotope records of the Toarcian Oceanic Anoxic Event (Early Jurassic) from North America and implications for the global drivers of the Toarcian carbon cycle. *Earth and Planetary Science Letters*, **459**, 118-126, https://doi.org/10.1016/j.epsl.2016.11.021
Them, T. R., Gill, B. C., Caruthers, A. H., Gerhardt, A. M., Gröcke, D. R., Lyons, T. W., Marroquín, S. M., Nielsen, S. G., Trabucho Alexandre, J. P. and Owens, J. D. 2018. Thallium isotopes reveal protracted anoxia during the Toarcian (Early Jurassic) associated with volcanism, carbon burial, and mass extinction. *Proceedings of the National Academy of Sciences*, **115**, 6596-6601, https://doi.org/10.1073/pnas.1803478115
Thierry, J. and Barrier, E. 2000. Middle Toarcian. *In*: Dercourt, J., Gaetani, M., Vrielynck, B., Barrier, E.B., Biju-Duval, B., Brunet, M.F., Cadet, J.P., Crasquin, S., Sandulescu, M. (Eds.), Atlas Peri-Tethys, Paleogeographic Maps. CCGM/CGMW, Map 8.
Trecalli, A., Spangenberg, J., Adatte, T., Föllmi, K.B. and Parente, M. 2012. Carbonate platform evidence of ocean acidification at the onset of the early Toarcian oceanic anoxic event. *Earth and Planetary Science Letters*, **357**, 214-225, https://doi.org/10.1016/j.epsl.2012.09.043
Ullmann, C.V., Thibault, N., Ruhl, M., Hesselbo, S.P. and Korte, C. 2014. Effect of a Jurassic oceanic anoxic event on belemnite ecology and evolution. *Proceedings of the National Academy of Sciences*, **111**, 10073-10076, https://doi.org/10.1073/pnas.1320156111
van Breugel, Y., Baas, M., Schouten, S., Mattioli, E., Sinninghe-Damste, J.S. 2006. Isorenieratane record in black shales from the Paris Basin, France: Constraints on recycling of respired CO_2 as a mechanism for negative carbon isotope shifts during the Toarcian oceanic anoxic event. *Paleoceanography*, **21**, PA4220, https://doi.org/10.1029/2006PA001305
van de Schootbrugge, B., Bailey, T.R., Rosenthal, Y., Katz, M.E., Wright, J.D., Miller, K.G., Feist-Burkhardt, S. and Falkowski, P.G. 2005. Early Jurassic climate change and the radiation

of organic-walled phytoplankton in the Tethys Ocean. *Paleobiology*, **31**, 73-97, https://doi.org/10.1666/0094-8373(2005)031%3C0073:ejccat%3E2.0.co;2

Vető, I., Demény, A., Hertelendi, E., Hetényi, M. 1997. Estimation of primary productivity in the Toarcian Tethys — a novel approach based on TOC, reduced sulphur and manganese contents. *Palaeogeography, Palaeoclimatology, Palaeoecology*, **132**, 355–371, https://doi.org/10.1016/s0031-0182(97)00053-9

Vörös, A. and Galácz, A. 1998. Jurassic palaeogeography of the Transdanubian Central Range (Hungary). *Rivista Italiana di Paleontologia e Stratigrafia*, **104**, 69-84.

Wohlwend, S., Hart, M.B. and Weissert, H. 2016. Chemostratigraphy of the Upper Albian to mid-Turonian Natih Formation (Oman) - how authigenic carbonate changes a global pattern. *The Depositional Record*, **2**, 97-117, https://doi.org/10.1002/dep2.15

Xu, W., Ruhl, M., Jenkyns, H.C., Hesselbo, S.P., Riding, J.B., Selby, D., Naafs, B.D.A., Weijers, J.W., Pancost, R.D., Tegelaar, E.W. and Idiz, E.F. 2017. Carbon sequestration in an expanded lake system during the Toarcian oceanic anoxic event. *Nature Geoscience*, **10**, 129-134, https://doi.org/10.1038/ngeo2871

Xu, W., Ruhl, M., Jenkyns, H.C., Leng, M.J., Huggett, J.M., Minisini, D., Ullmann, C.V., Riding, J.B., Weijers, J.W., Storm, M.S., Percival, L.M., Tosca, N.J., Idiz, E.F., Tegelaar, E.W., and Hesselbo, S.P. 2018. Evolution of the Toarcian (Early Jurassic) carbon-cycle and global climatic controls on local sedimentary processes (Cardigan Bay Basin, UK). *Earth and Planetary Science Letters*, **484**, 396-411, https://doi.org/10.1016/j.epsl.2017.12.037

Tables

	$\delta^{13}C$ and $\delta^{18}O$		$\delta^{13}C$ and Sr/Ca		$\delta^{18}O$ and Sr/Ca	
	Pearson (r)	**p-value**	**Pearson (r)**	**p-value**	**Pearson (r)**	**p-value**
Kisgerecse:						
Törökbükk Lst. Fm.	0,03	0,39	-0,46	0,075	-0,32	0,18
Kisgerecse M. Fm.	0,51	0,0038	-0,35	0,051	-0,05	0,38
Tölgyhát:						
Törökbükk Lst. Fm.	0,60	0,00051	-0,25	0,147	-0,38	0,04
Úrkút M. Fm.	0,87	0,0026	0,08	0,374	0,22	0,32
Kisgerecse M. Fm.	-0,50	0,072	-0,62	0,022	0,47	0,09

Table 1 – Pearson correlation values (r) of $\delta^{13}C$, $\delta^{18}O$ and Sr/Ca ratios and their statistical significance (p) by sections and formations.

Label	Sample	Height (cm)	*Schizosphaerella*	*Mitrolithus jansae*	*Mitrolithus elegans*	*Crepidolithus crassus*	*Tubirhabdus patulus*	*Similiscutum finchii*	large *Similiscutum finchii*	*Similiscutum novum*	*Lotharingius crucicentralis*	*Lotharingius frodoi*	*Lotharingius hauffii*	*Lotharingius sigillatus*	*Lotharingius umbriensis*	*Discorhabdus ignotus*	*Discorhabdus striatus*	large *Calyculus*	unidentified coccolith	preservation	**Nannofossil zone**	**Age**
TH	210	270	.	.	.	•	.	.	.	•	.	•	•	.	.	•	•	.	.	VVP	NJT7a	early-middle Toarcian
TH	166	226																		B		
TH	163	223	.	.	.	•	.	.	.	.	.	.	.	•	.	.	• =	.	.	VVP		
TH	151	211	.	.	.	•	.	.	.	.	.	.	.	.	.	.	.	.	.	VVP	NJT6b	early Toarcian
TH	120	180		=																B		
TH	100	160	.	•	.	.	.	.	.	.	.	•	.	.	.	.	.	•	•	VVP	?	
TH	73	133	•	.	.	•	•	•	•	.	.	•	•	.	.	•	.	•	.	VVP		
TH	60	120	•	•	•	•	•	.	.	•	.	•	•	•	•	•	.	.	.	VVP		
TH	33	93																		B		
TH	19	79																		B		
TH	12G	72	•																	VVP		
TH	9	69																		BB		
TH	8	68	•																	nB		
TH	5	65	•	.	.	.	.	.	.	.	• –	.	.	•	.	.	.	.	.	VVP	NJT5b	late Pliensbachian
TH	0	60	•																	nB	?	
TH	-30	30	•																	nB		
TH	-60	0	•	•	•	•	.	.	.	•	.		•	.	•	.	.	.	•	VVP		

Nannofossil data
- • present
- . absent
- = last occurrence
- = first occurrence
- – presence

Preservation
VVP = extremely poor
B = barren sample
nB = nearly barren

Table 2 – Distribution of nannofossil taxa in the Tölgyhát section.

Figure captions

Fig 1 – A: Paleogeographic map of Europe and the NW Tethys during the Early Jurassic (modified from Thierry and Barrier, 2000). Positions of the NW Tethyan tectonic units (TRU: Transdanubian Range Unit, Austro-Alpine Units, WCU: Western Carpathian Units and Tisza Unit; supposed areas marked with dashed line). Modified from Häusler et al. (1993) and Haas (2012). B: Close-up view of the NW Tethyan margin during the Early Jurassic.

Fig 2 – A: Locations of the studied sections and map of sedimentary facies of the Toarcian deposits in the Transdanubian Range (after Vörös & Galácz, 1998). B: Upper Pliensbachian and lower Toarcian pelagic succession exposed in an abandoned quarry at Tölgyhát. C: Uppermost Pliensbachian beds of the Törökbükk Formation from the Kisgerecse section. D: Trench exploring the lower Toarcian Kisgerecse Formation at the Kisgerecse section.

Fig 3 – Litho- and chronostratigraphic chart of the uppermost Triassic and Lower Jurassic formations in the Gerecse Hills and adjacent areas in the Transdanubian Range Unit, along a SW to NE transect. Colours approximate the appearance of these rocks in the field. The chart and inferred depositional environments are adapted from Főzy (2012) and Budai et al. (2018). Lst. – limestone, Fm. – Formation.

Fig 4 – Lithological log and geochemical data obtained from the Tölgyhát section. Ammonite biostratigraphy after Géczy (1984, 1985). Nannofossil biostratigraphy is from this study. Lst. – Limestone. Fm. – Formation. Bif. – Bifrons Zone.

Fig 5 – Lithological log and geochemical data obtained from the Kisgerecse section. Ammonite biostratigraphy after Géczy, 1984; 1985 and Kovács, 2012. Grey curve: carbonate carbon isotope record from Jenkyns et al., 1991. Törökb. Fm. – Törökbükk Limestone Formation. Fm. – Formation. Eman. – Emaciatum Zone. T. – Tenuicostatum Zone. Serp. – Serpentinum Subzone.

Fig 6 – Scatter plots of carbon and oxygen isotope and Sr/Ca ratios from the Tölgyhát and Kisgerecse sections for diagenetic screening.

Fig 7 – Mineral composition of sampled layers in the Tölgyhát section.

Fig 8 – Chemostratigraphic correlation of the Tölgyhát and Kisgerecse sections with the continuous reference record of the Toarcian GSSP section at Peniche, Portugal. $\delta^{13}C$ curve and stratigraphic scale for Peniche is from Hesselbo et al. (2007). Nannofossil biostratigraphy of Peniche from Ferreira et al. (2019). Astrochronology from Huang & Hesselbo (2014). Ammonite biostratigraphy for the Tölgyhát section from Géczy (1984), calcareous nannofossils from this study. Ammonite biostratigraphy of the Kisgerecse section from Géczy (1984; 1985) and Kovács (2012). Grey curve: bulk carbon isotope data by Jenkyns et al. (1991).

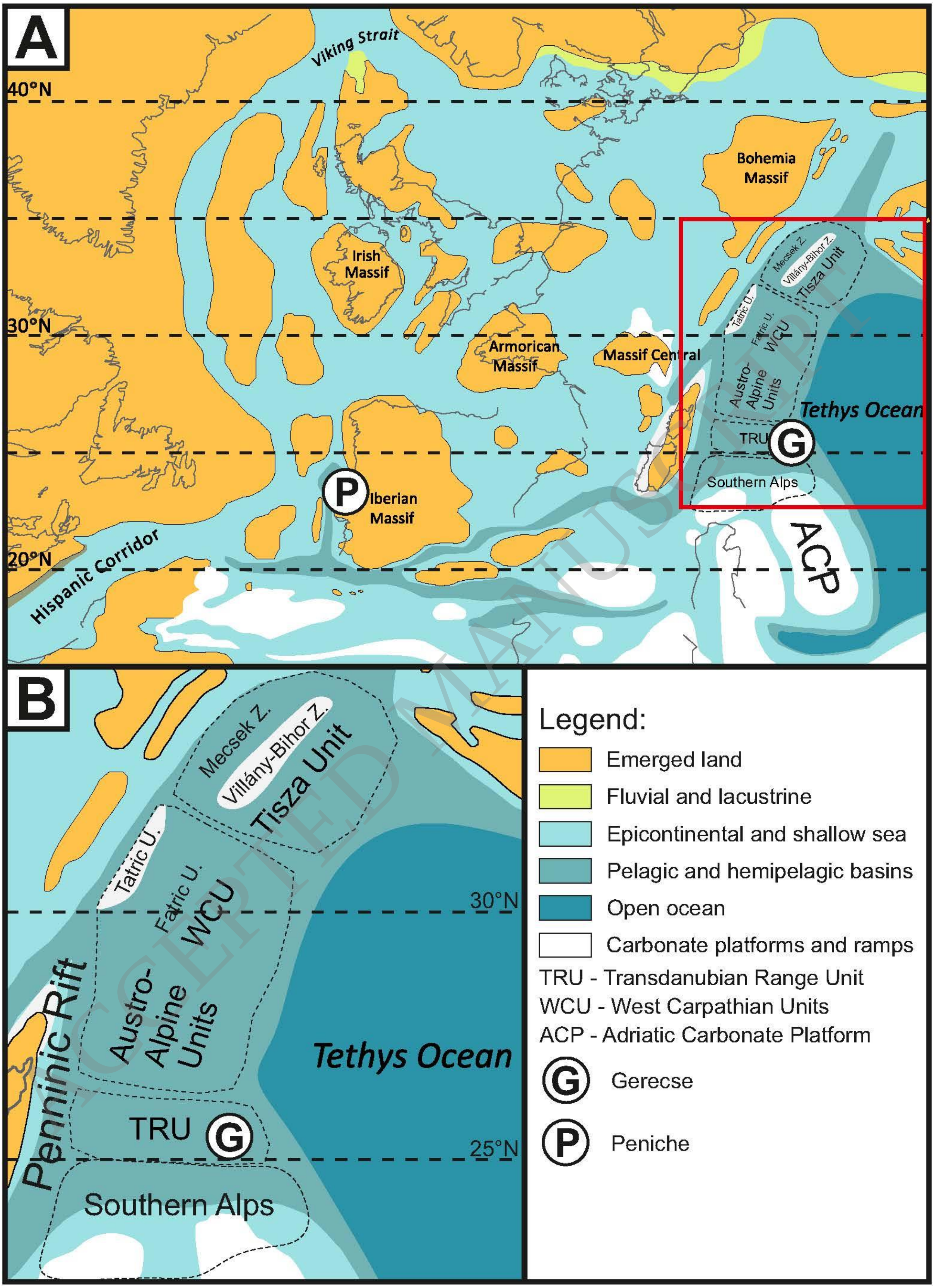
A
40°N
30°N
20°N
Viking Strait
Bohemia Massif
Irish Massif
Armorican Massif
Massif Central
Iberian Massif
Hispanic Corridor
Tethys Ocean
Mecsek Z.
Villány-Bihor Z.
Tisza Unit
Tatric U.
Fatric U.
WCU
Austro-Alpine Units
TRU
Southern Alps
ACP
P
G
B
30°N
25°N
Penninic Rift
Legend:
Emerged land
Fluvial and lacustrine
Epicontinental and shallow sea
Pelagic and hemipelagic basins
Open ocean
Carbonate platforms and ramps
TRU - Transdanubian Range Unit
WCU - West Carpathian Units
ACP - Adriatic Carbonate Platform
Gerecse
Peniche

Figure 1

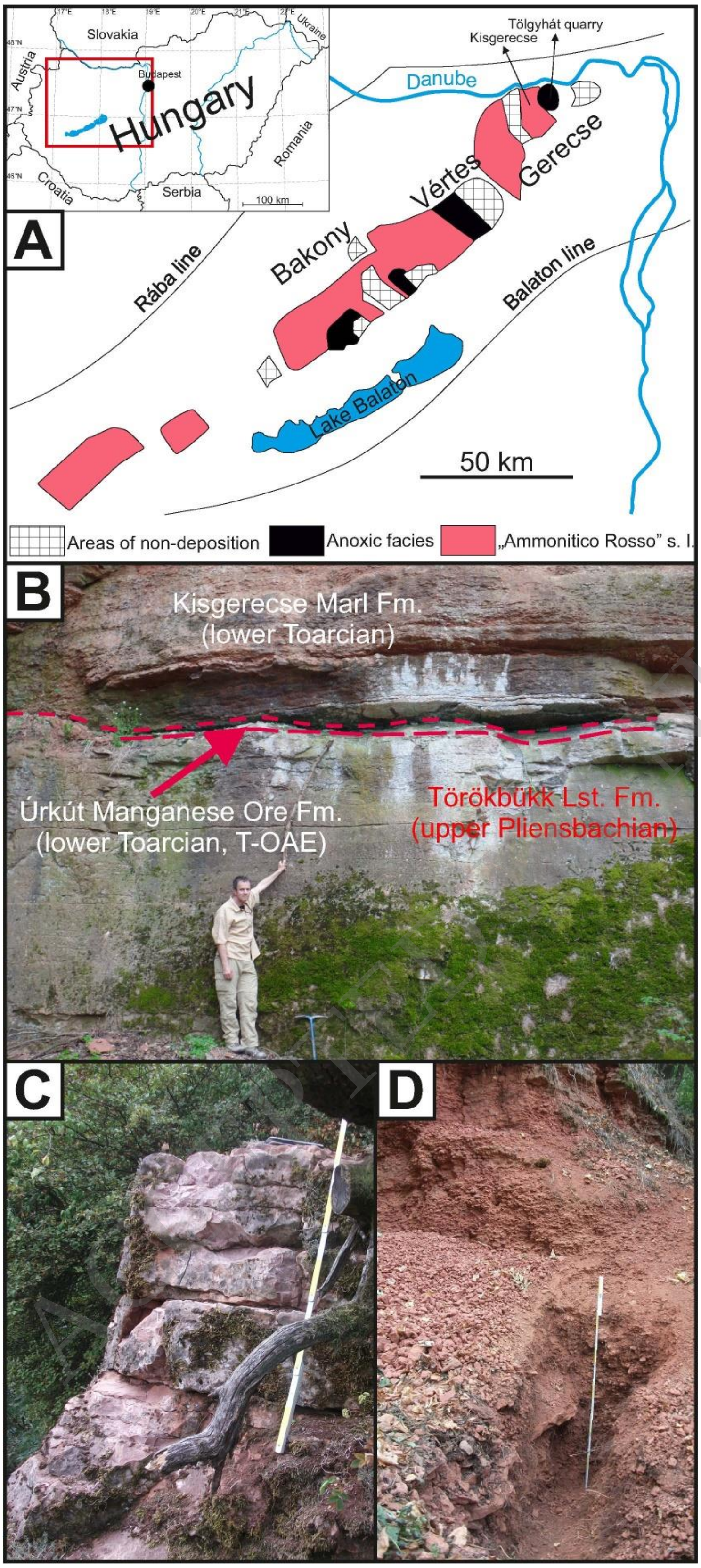
A
17°E
18°E
19°E
20°E
21°E
22°E
48°N
47°N
46°N
Slovakia
Ukraine
Austria
Budapest
Hungary
Romania
Croatia
Serbia
100 km
Tölgyhát quarry
Kisgerecse
Danube
Gerecse
Vértes
Bakony
Rába line
Balaton line
Lake Balaton
50 km
Areas of non-deposition
Anoxic facies
„Ammonitico Rosso" s. l.
B
Kisgerecse Marl Fm.
(lower Toarcian)
Úrkút Manganese Ore Fm.
(lower Toarcian, T-OAE)
Törökbükk Lst. Fm.
(upper Pliensbachian)
C
D

Figure 2

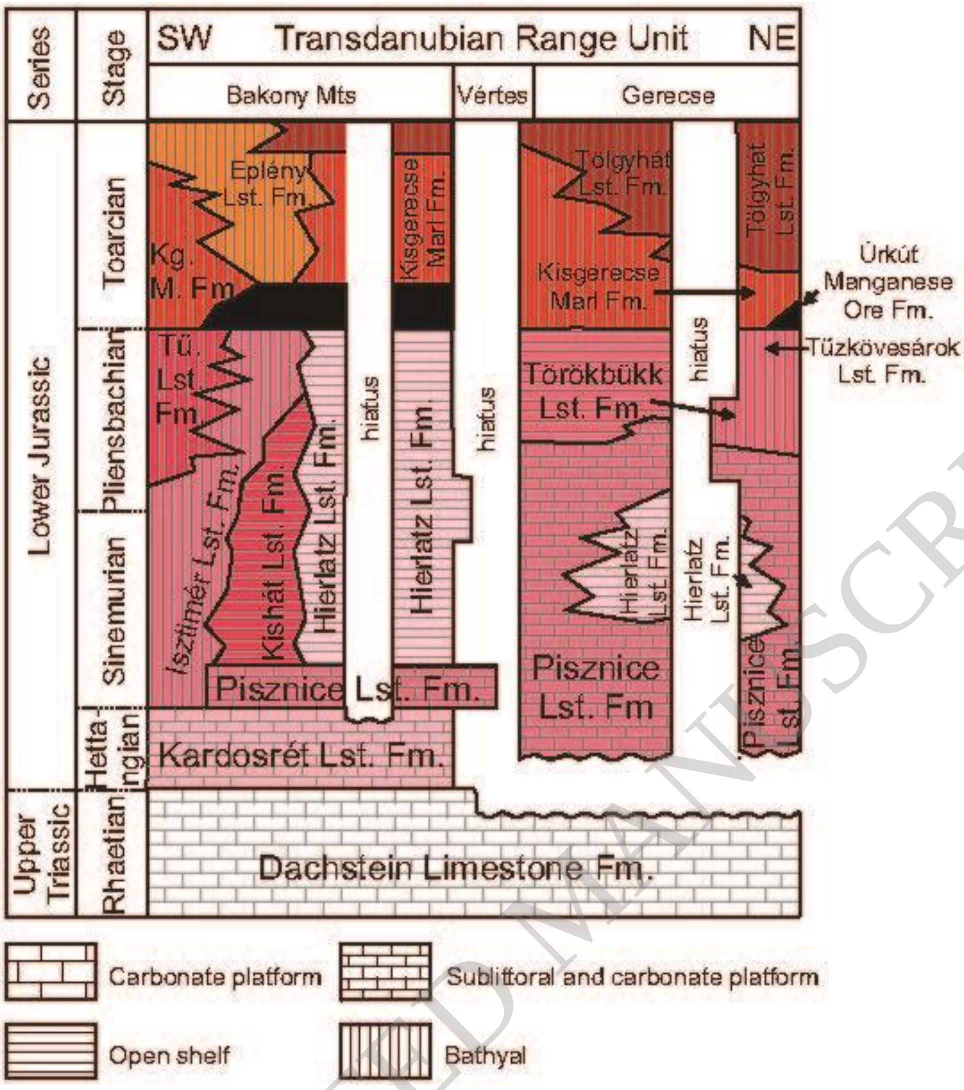

Series
Stage
SW
Transdanubian Range Unit
NE
Bakony Mts
Vértes
Gerecse
Lower Jurassic
Upper Triassic
Toarcian
Pliensbachian
Sinemurian
Hettangian
Rhaetian
Eplény Lst. Fm.
Kg. M. Fm.
Kisgerecse Marl Fm.
Tölgyhát Lst. Fm.
Kisgerecse Marl Fm.
Tölgyhát Lst. Fm.
Úrkút Manganese Ore Fm.
Tüzkövesárok Lst. Fm.
Tü. Lst. Fm.
Isztimér Lst. Fm.
Kisház Lst. Fm.
Hierlatz Lst. Fm.
hiatus
Hierlatz Lst. Fm.
hiatus
Törökbükk Lst. Fm.
hiatus
Hierlatz Lst. Fm.
Hierlatz Lst. Fm.
Pisznice Lst. Fm.
Pisznice Lst. Fm.
Pisznice Lst. Fm.
Kardosrét Lst. Fm.
Dachstein Limestone Fm.
Carbonate platform
Sublittoral and carbonate platform
Open shelf
Bathyal

Figure 3

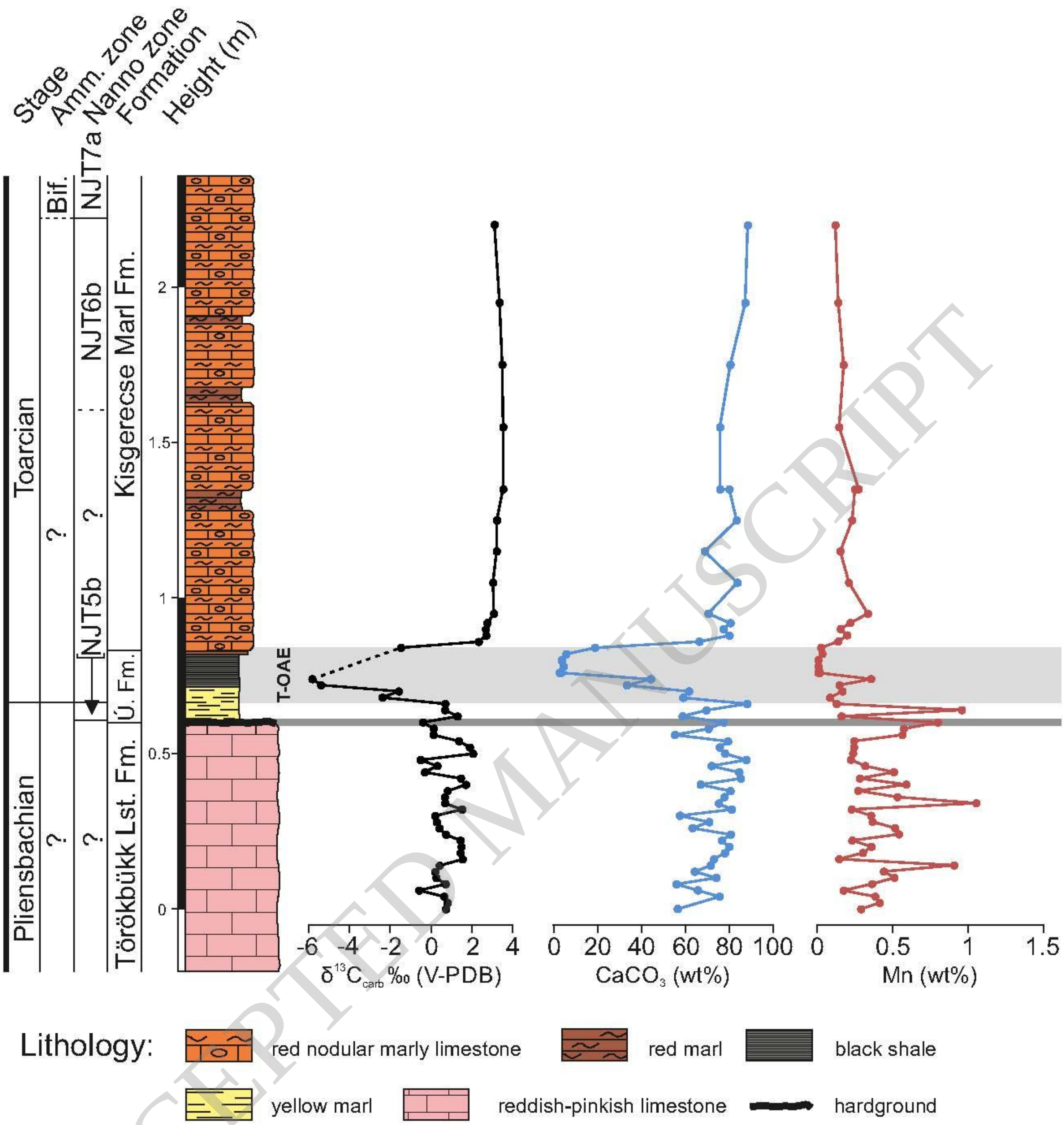

Stage
Amm. zone
Nanno zone
Formation
Height (m)
Toarcian
Pliensbachian
Bif.
NJT7a
NJT6b
NJT5b
Kisgerecse Marl Fm.
Ú. Fm.
Törökbükk Lst. Fm.
T-OAE
δ13Ccarb ‰ (V-PDB)
CaCO3 (wt%)
Mn (wt%)
Lithology:
red nodular marly limestone
red marl
black shale
yellow marl
reddish-pinkish limestone
hardground

Figure 4

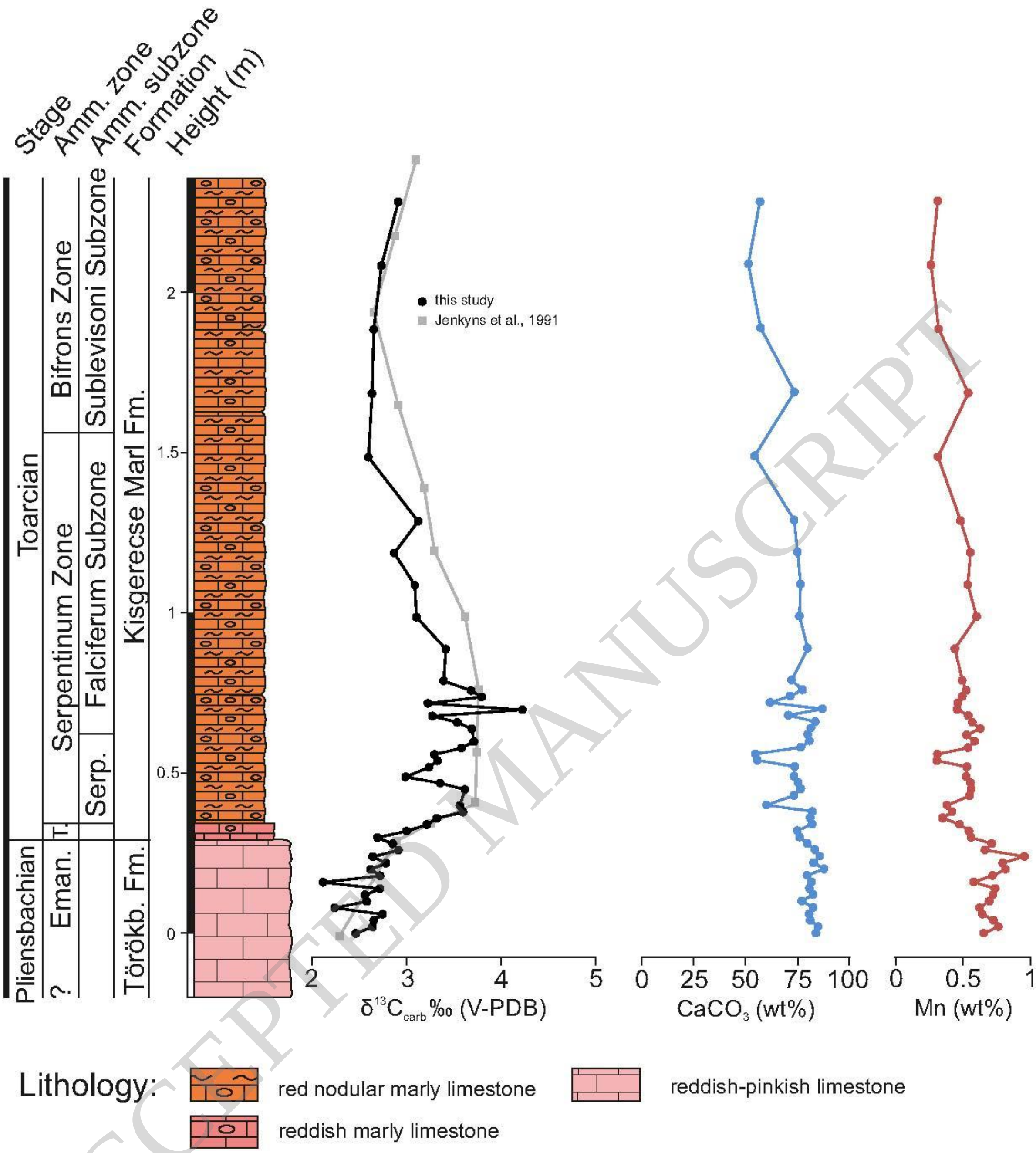
Stage
Amm. zone
Amm. subzone
Formation
Height (m)
Toarcian
Pliensbachian
Bifrons Zone
Serpentinum Zone
Eman.
T.
?
Sublevisoni Subzone
Falciferum Subzone
Serp.
Kisgerecse Marl Fm.
Törökb. Fm.
this study
Jenkyns et al., 1991
δ13Ccarb ‰ (V-PDB)
CaCO3 (wt%)
Mn (wt%)
Lithology:
red nodular marly limestone
reddish marly limestone
reddish-pinkish limestone

Figure 5

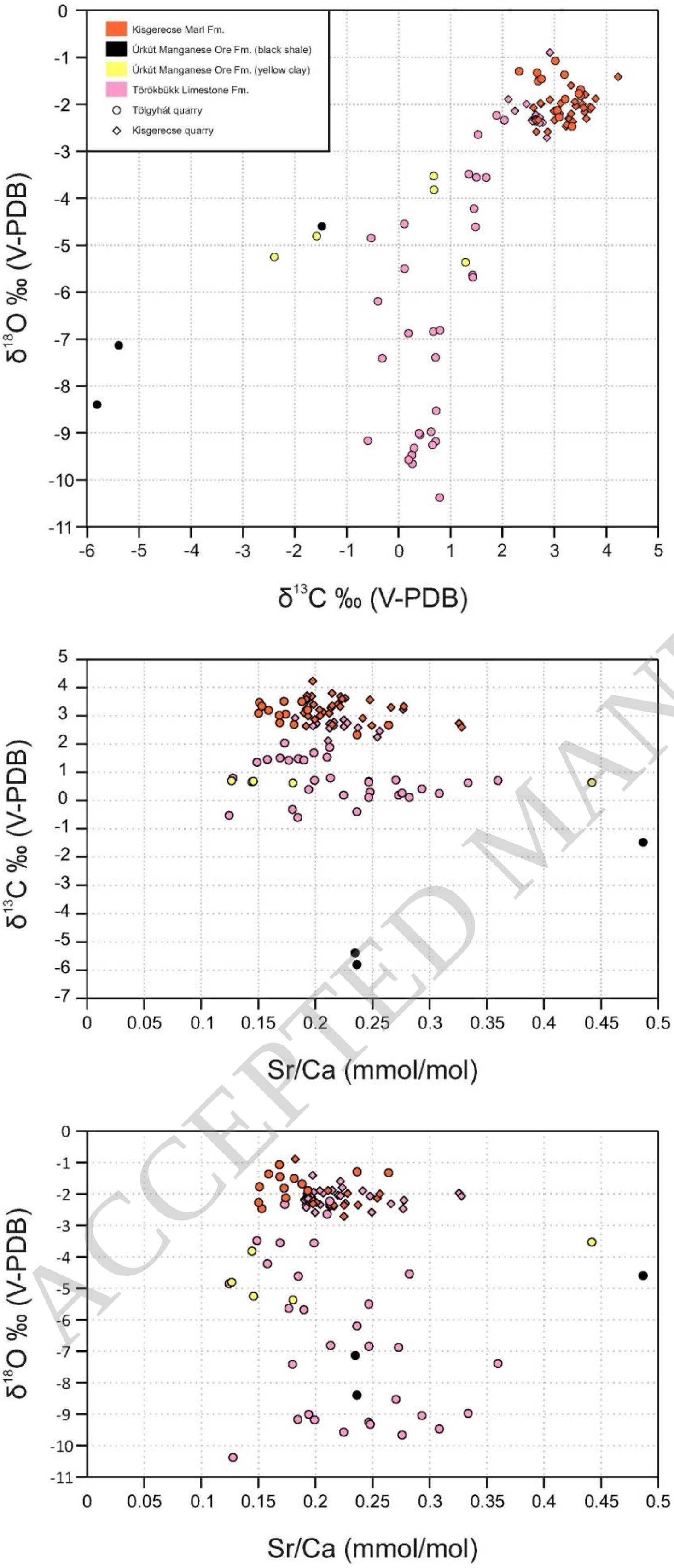
Kisgerecse Marl Fm.
Úrkút Manganese Ore Fm. (black shale)
Úrkút Manganese Ore Fm. (yellow clay)
Törökbükk Limestone Fm.
Tölgyhát quarry
Kisgerecse quarry
δ18O ‰ (V-PDB)
δ13C ‰ (V-PDB)
δ13C ‰ (V-PDB)
Sr/Ca (mmol/mol)
δ18O ‰ (V-PDB)
Sr/Ca (mmol/mol)

Figure 6

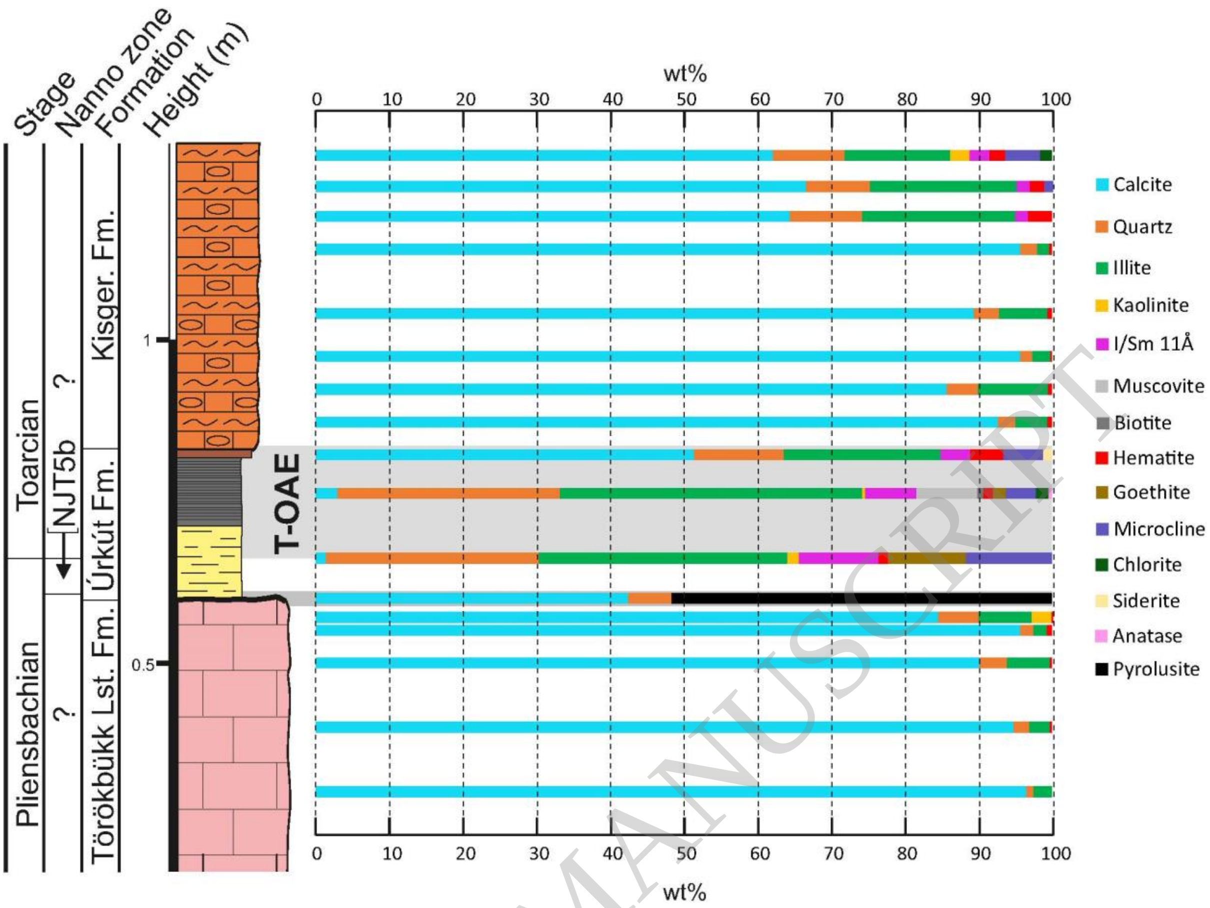

Stage
Nanno zone
Formation
Height (m)
wt%
0
10
20
30
40
50
60
70
80
90
100
Toarcian
Pliensbachian
?
NJT5b
?
Kisger. Fm.
Úrkút Fm.
Törökbükk Lst. Fm.
1
0.5
T-OAE
Calcite
Quartz
Illite
Kaolinite
I/Sm 11Å
Muscovite
Biotite
Hematite
Goethite
Microcline
Chlorite
Siderite
Anatase
Pyrolusite

Figure 7

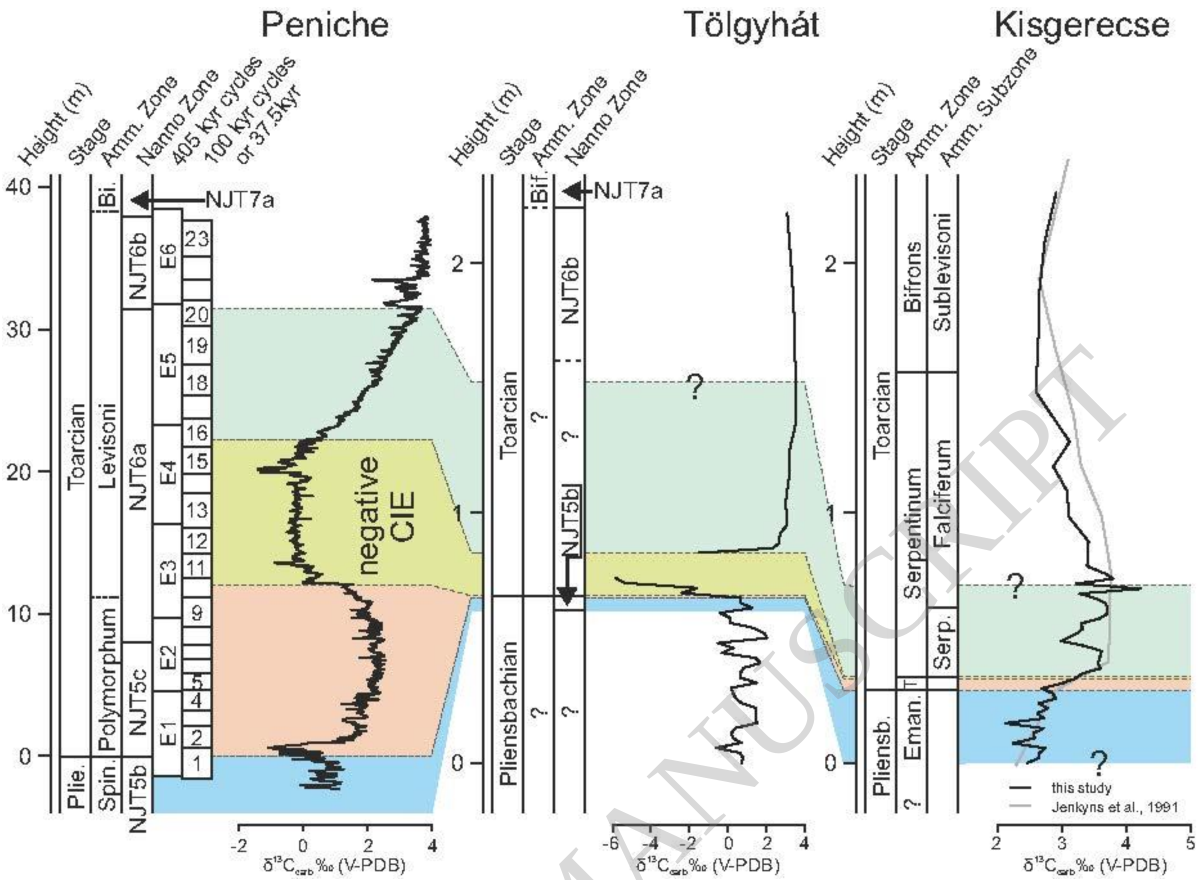
Peniche
Tölgyhát
Kisgerecse
Height (m)
Stage
Amm. Zone
Nanno Zone
405 kyr cycles
100 kyr cycles or 37.5kyr
NJT7a
negative CIE
Toarcian
Pliensbachian
Levisoni
Polymorphum
Spin.
Plie.
Bi.
Bif.
NJT6b
NJT6a
NJT5c
NJT5b
NJT5bl
Amm. Subzone
Bifrons
Sublevisoni
Serpentinum
Falciferum
Serp.
Pliensb.
Eman.
this study
Jenkyns et al., 1991
δ13Ccarb‰ (V-PDB)

Figure 8